



Munich Personal RePEc Archive

A New Approach to Infer Changes in the Synchronization of Business Cycle Phases

Leiva-Leon, Danilo

Bank of Canada

17 June 2013

Online at <https://mpra.ub.uni-muenchen.de/54452/>
MPRA Paper No. 54452, posted 19 Mar 2014 07:27 UTC

A New Approach to Infer Changes in the Synchronization of Business Cycle Phases*

Danilo Leiva-Leon[†]
Bank of Canada

Abstract

This paper proposes a Markov-switching framework useful to endogenously identify regimes where economies enter recessionary and expansionary phases synchronously, and regimes where economies are unsynchronized following independent business cycle phases. The reliability of the framework to track synchronization changes is corroborated with Monte Carlo experiments. An application to the case of U.S. states reports substantial changes over time in the cyclical affiliation patterns of states. Moreover, a network analysis discloses a change in the propagation pattern of aggregate contractionary shocks across states, suggesting that regional economies in U.S. have become more interdependent since the early 90s.

Keywords: Business Cycles, Markov-Switching, Network Analysis.

JEL Classification: E32, C32, C45.

*I especially thank Maximo Camacho, Marcelle Chauvet, James D. Hamilton and Gabriel Perez-Quiros for their helpful comments and suggestions. I also benefited from conversations with James Morley and Michael T. Owyang. Thanks to the seminar participants at the Bank of Canada, Bank of Mexico, Central Bank of Chile and the University of California Riverside, and conference participants at the 6th CSDA International Conference on Computational and Financial Econometrics, the 12th Annual Missouri Economics Conference and the XXXVII Symposium of the Spanish Economic Association. A preliminary version of this paper circulated under the name "Monitoring Synchronization of Regional Recessions: A Markov-Switching Network Approach." Supplementary material of this paper can be found at the author's webpage: <https://sites.google.com/site/daniloleivaleon/media>. The views expressed in this paper are those of the author(s) and do not represent the views of the Bank of Canada.

[†]International Economic Analysis Department, Bank of Canada, 234 Laurier Avenue West, Ottawa, Ontario, Canada, K1A 0G9. E-mail: leiv@bankofcanada.ca

1 Introduction

The analysis of business cycles synchronization provides crucial information for policy makers in determining the regions, in the case of a country, or the countries, in the case of a union, more sensitive to economic policies or aggregate economic shocks. Most of the related studies have mainly focused on describing economies' cyclical association patterns during a given time span, however few has been done in assessing potential changes in those patterns occurred during such time span, which can be caused by a variety of reasons, such as policy changes, trade agreements, economic unions, aggregate recessionary shocks, etc.

Due to the asymmetric nature of business cycles, multivariate Markov-switching (MS) models have become a useful tool in analyzing the synchronization of countries, Smith and Summers (2005), Camacho and Perez-Quiros (2006), among others, or the regions of a country, Owyang et al. (2005) and Hamilton and Owyang (2012). In these studies, real economic activity is modeled as a function of a latent variable which indicates, at each time period, if the economy is in a recessionary or in an expansionary phase. These studies provide an overall picture about the synchronization between the business cycles phases of different economies, although they are not able to endogenously identify potential synchronization changes. This is because, in order to preserve parsimony in the models, a non-explored question that could help to unveil this feature has remained unnoticed: how does the dependency relationship between the latent variables governing a multivariate MS model vary over time?

The approaches used in the literature to deal with multivariate MS frameworks traditionally assume constant dependency relationships between the latent variables, which can be sorted into two categories. The first one refers to studies where such relation is just *a priori* assumed based on the researcher's judgment. Multivariate MS models are usually analyzed under three different settings, Hamilton and Lin (1996) and Anas et al. (2007). The first one refers to the case where all series follow common regime dynamics, Krolzig (1997) and Sims and Zha (2006). Second, the use of totally independent Markov chains, which is the most followed approach, Smith and Summers (2005) and Chauvet and Senyuz (2008). Third, the dynamics of one latent variable precedes those of other latent variables, Hamilton and Perez-Quiros (1996) and Cakmakli et al. (2011), which allows for possibly different number of lags.¹ Accordingly, the obtained regime inferences and final interpretations of the model's output may substantially vary depending on the type of judgment. There is also the case of a general Markovian specification which involves

¹Another type of relationship, under a univariate framework, is presented in Bai and Wang (2011) where the state variable governing the mean of the process is conditional to the one governing the variance of such process.

the full transition probability matrix, however, it brings computational difficulties as the model increases in the number of series, states or lags, becoming also less straightforward to interpret, and moreover, it does not allow to endogenously infer the type of relationship between the latent variables.

The second category focuses on making *a posteriori* assessments of the synchronization between MS processes, providing "average" dependency relationship estimates. Works in this line are Guha and Banerji (1998) and Artis et al. (2004), which after estimating different univariate models, compute cross-correlations between the probabilities of being in recession as measure of synchronization. However, as shown in Camacho and Perez-Quiros (2006), these approaches may lead to misleading results since they are biased to show relatively low values of synchronization precisely for countries that exhibit synchronized cycles. This suggests that a bivariate framework would provide a better characterization of pairwise synchronization than two univariate models.

Regarding the analysis of pairwise business cycle contemporaneous synchronization, Phillips (1991) point out the two extreme cases presented in the literature; the case of complete independence (two independent Markov processes are hidden in the bivariate specification) and the case of perfect synchronization (only one Markov process for both variables). In this line, Harding and Pagan (2006) propose a test for the hypotheses that cycles are either unsynchronized or perfectly synchronized, also Pesaran and Timmermann (2009) focus on testing independence between discrete multicategory variables based on canonical correlations. Another similar approach followed by Camacho and Perez-Quiros (2006), Bengoechea et al. (2006), and Leiva-Leon (2014), consists on modeling the data generating process as a linear combination between the unsynchronized and perfectly synchronized cases. Despite the fact that these approaches provide inference on the dependency relationship among the latent variables, they are not able to analyze it in a time-varying fashion.

This paper provides a new approach to infer the time-varying relationship between the latent variables governing multivariate MS models. This information allows to endogenously identify regimes where two economies enter recessions and expansions synchronously, from regimes where the economies are unsynchronized, experimenting independent business cycle phases. In contrast to the previous related literature, the proposed filter not only provides a full characterization of the regime inferences, but simultaneously also provides inferences on the type of synchronicity that both economies experience at each period of time.

The model is estimated by Gibbs sampling and its reliability is assessed with Monte Carlo experiments, finding it a suitable approach to track changes in the synchronization of cycles. Moreover, the obtained pairwise synchronizations can be easily converted into dissimilarity measures, which can be interpreted as cyclical distances and used in assessing

changes in the clustering and interdependence patterns that could experiment, not only two, but many economies. This is done by relying on network analysis, where economies take the interpretation of nodes and links between pairs of nodes are given by the estimated synchronicity, fully characterizing a business cycle network governed by Markovian dynamics.

The proposed framework is applied to investigate potential variations in the cyclical interdependence between the states of U.S., obtaining three main findings. First, the results report the existence of interdependence cycles which are associated to NBER recessions, such cycles are defined as periods characterized by low cyclical heterogeneity across states, experienced during the recessionary and recovery phases, followed by longer periods of high cyclical heterogeneity, occurred during the phases of stable growth. Second, there are substantial variations in the grouping pattern of states over time, going from a scheme characterized by several clusters of states to a core and periphery structure, composed by highly and lowly synchronized states, respectively. Third, the network analysis documents a change in the propagation pattern of contractionary shocks across states, which consist on going from recessions characterized by shocks being spread mainly toward few but big states in GDP share terms, until the nineties, to recessions where shocks have been more uniformly spread to all states, after that time, suggesting that U.S. economy's regions have become more interdependent since the early 90s.

The paper is structured as follows. Section 2 presents the proposed time-varying synchronization approach, describes the filtering algorithm and reports the Monte Carlo simulation results. Section 3 analyzes the dynamic synchronization of business cycle phases in U.S. states, by relying on bivariate, multivariate and network analyses. Finally, Section 4 concludes.

2 The Model

Let $y_{i,t}$ be the growth rate of an economic activity index of economy i , which can be modeled as a function of a latent or unobserved state variable, $S_{i,t}$, which indicates if such economy is in a recessionary or expansionary regime, an idiosyncratic component, $\epsilon_{i,t}$, and a set of additional parameters, θ_i . Accordingly, for $i = a, b$,

$$y_{a,t} = f(S_{a,t}, \epsilon_{a,t}, \theta_a) \tag{1}$$

$$y_{b,t} = f(S_{b,t}, \epsilon_{b,t}, \theta_b), \tag{2}$$

the goal of this section is to provide assessments on the synchronization between $S_{a,t}$ and $S_{b,t}$ for each period of time, that is,

$$sync(S_{a,t}, S_{b,t}) = \Pr(S_{a,t} = S_{b,t}), \text{ for } t = 1, \dots, T \tag{3}$$

Following the line of Owyang et al. (2005) and in Hamilton and Owyang (2012), who rely on AR(0) MS specification, I consider the following tractable bivariate two-state Markov-switching specification:

$$\begin{bmatrix} y_{a,t} \\ y_{b,t} \end{bmatrix} = \begin{bmatrix} \mu_{a,0} + \mu_{a,1}S_{a,t} \\ \mu_{b,0} + \mu_{b,1}S_{b,t} \end{bmatrix} + \begin{bmatrix} \varepsilon_{a,t} \\ \varepsilon_{b,t} \end{bmatrix}, \quad \begin{bmatrix} \varepsilon_{a,t} \\ \varepsilon_{b,t} \end{bmatrix} \sim N \left(\begin{bmatrix} 0 \\ 0 \end{bmatrix}, \begin{bmatrix} \sigma_a^2 & \sigma_{ab} \\ \sigma_{ab} & \sigma_b^2 \end{bmatrix} \right). \quad (4)$$

It is worth to note that the results derived in this section can be straightforwardly extended to specifications including lags in the dynamics, however Camacho and Perez-Quiros (2007) show that positive autocorrelation existing in macroeconomic time series can be better captured by shifts between business cycle states rather than by the standard view of autoregressive coefficients. The model can also be extended to allow for regime switching in the variance-covariance matrix, however since the empirical application focuses on the period after the Great Moderation, such feature is not included in the model.

The state variable $S_{k,t}$ indicates that y_{kt} is in regime 0 with a mean equal to $\mu_{k,0}$, when $S_{k,t} = 0$, or that y_{kt} is in regime 1 with a mean equal to $\mu_{k,0} + \mu_{k,1}$, when $S_{k,t} = 1$, for $k = a, b$. Moreover $S_{a,t}$ and $S_{b,t}$ evolve according to irreducible two-state Markov chains, whose transition probabilities are given by

$$\Pr(S_{k,t} = j | S_{k,t-1} = i) = p_{k,ij}, \text{ for } i, j = 0, 1 \text{ and } k = a, b. \quad (5)$$

To characterize the dynamics of $y_t = [y_{a,t}, y_{b,t}]'$, the information contained in $S_{a,t}$ and $S_{b,t}$ can be summarized in the state variable, $S_{ab,t}$, which accounts for the possible combinations that the vector, $\mu_{S_{ab,t}} = [\mu_{a,0} + \mu_{a,1}S_{a,t}, \mu_{b,0} + \mu_{b,1}S_{b,t}]'$, could take trough the different regimes.

$$S_{ab,t} = \begin{cases} 1, & \text{If } S_{a,t} = 0, S_{b,t} = 0 \\ 2, & \text{If } S_{a,t} = 0, S_{b,t} = 1 \\ 3, & \text{If } S_{a,t} = 1, S_{b,t} = 0 \\ 4, & \text{If } S_{a,t} = 1, S_{b,t} = 1 \end{cases}. \quad (6)$$

Following the line of Harding and Pagan (2006), the objective of the propose model is to differentiate regimes where the phases of $y_{a,t}$ and $y_{b,t}$ are unsynchronized, implying that $S_{a,t}$ and $S_{b,t}$ follow independent dynamics, that is

$$\Pr(S_{a,t} = j_a, S_{b,t} = j_b) = \Pr(S_{a,t} = j_a) \Pr(S_{b,t} = j_b), \quad (7)$$

from regimes where the phases of $y_{a,t}$ and $y_{b,t}$ are fully synchronized, entering expansions and recessions synchronously, implying that $S_{a,t} = S_{b,t} = S_t$, that is

$$\Pr(S_{a,t} = j_a, S_{b,t} = j_b) = \Pr(S_t = j). \quad (8)$$

In order to do so, I introduce into the framework another latent variable, V_t , that takes the value of 1 if business cycle phases are in a synchronized regime, and the value of 0 if they are under an unsynchronized regime at time t , that is

$$V_t = \begin{cases} 0 & \text{If } S_{a,t} \text{ and } S_{b,t} \text{ are unsynchronized} \\ 1 & \text{If } S_{a,t} \text{ and } S_{b,t} \text{ are synchronized} \end{cases}. \quad (9)$$

The latent variable V_t also evolves according to an irreducible two-state Markov chain whose transition probabilities are given by

$$\Pr(V_t = j_v | V_{t-1} = i_v) = p_{v,kl}, \quad \text{for } i_v, j_v = 0, 1. \quad (10)$$

The advantage of introducing, V_t , rather than analyzing the general Markovian specification with the full transition probability matrix, as in Sims et al. (2008), is that all the information about the dependency relationship between the latent variables remains summarized in a single variable, V_t , providing an easy to interpret way of assessing sync changes and being able even to provide information of the expected duration of regimes were economies are synchronized or unsynchronized based on its associated transition probabilities. Notice that the analysis in this paper focuses on dependency, not on correlations, since the objective is to determine if two economies are either synchronized or unsynchronized.

Accordingly, there is an enlargement of the set of regimes in Equation (6) which remains fully characterized by the latent variable $S_{ab,t}^*$, that simultaneously collects information regarding to joint dynamics, individual dynamics and their dependency relationship over time,

$$S_{ab,t}^* = \begin{cases} 1, & \text{If } S_{a,t} = 0, S_{b,t} = 0, V_t = 0 \\ 2, & \text{If } S_{a,t} = 0, S_{b,t} = 1, V_t = 0 \\ 3, & \text{If } S_{a,t} = 1, S_{b,t} = 0, V_t = 0 \\ 4, & \text{If } S_{a,t} = 1, S_{b,t} = 1, V_t = 0 \\ 5, & \text{If } S_{a,t} = 0, S_{b,t} = 0, V_t = 1 \\ 6, & \text{If } S_{a,t} = 0, S_{b,t} = 1, V_t = 1 \\ 7, & \text{If } S_{a,t} = 1, S_{b,t} = 0, V_t = 1 \\ 8, & \text{If } S_{a,t} = 1, S_{b,t} = 1, V_t = 1 \end{cases}, \quad (11)$$

Inferences on the latent variable $S_{ab,t}^*$, can be computed by conditioning on V_t ,²

$$\begin{aligned} \Pr(S_{ab,t}^* = j_{ab}^*) &= \Pr(S_{a,t} = j_a, S_{b,t} = j_b, V_t = j_v) \\ &= \Pr(S_{a,t} = j_a, S_{b,t} = j_b | V_t = j_v) \Pr(V_t = j_v) \end{aligned} \quad (12)$$

²Notice that states 6 and 7 in Equation (11) are truncated to zero by construction, since the two state variables cannot be in different states if they are perfectly synchronized, i.e. $\Pr(S_{a,t} = j_a, S_{b,t} = j_b | V_t = 1) = 0$ for any $j_a \neq j_b$.

where $\Pr(S_{a,t} = j_a, S_{b,t} = j_b | V_t = j_v)$ indicates the inferences on the dynamics of $S_{ab,t}$ conditional on total independence, if $V_t = 0$, or conditional on full dependence, if $V_t = 1$. In the former case the joint probability of $S_{ab,t}^*$ is given by

$$\begin{aligned} \Pr(S_{a,t} = j_a, S_{b,t} = j_b, V_t = 0) &= \Pr(S_{a,t} = j_a, S_{b,t} = j_b | V_t = 0) \Pr(V_t = 0) \\ &= \Pr(S_{a,t} = j_a) \Pr(S_{b,t} = j_b) \Pr(V_t = 0), \end{aligned} \quad (13)$$

while in the latter case it is

$$\begin{aligned} \Pr(S_{a,t} = j_a, S_{b,t} = j_b, V_t = 1) &= \Pr(S_{a,t} = j_a, S_{b,t} = j_b | V_t = 1) \Pr(V_t = 1) \\ &= \Pr(S_t = j) \Pr(V_t = 1). \end{aligned} \quad (14)$$

Therefore, inferences on the state variable $S_{ab,t}$, in Equation (6), after accounting for synchronization, can be easily recovered by integrating $\Pr(S_{a,t} = j_a, S_{b,t} = j_b, V_t = j_v)$ through V_t , remaining as

$$\begin{aligned} \Pr(S_{a,t} = j_a, S_{b,t} = j_b) &= \Pr(V_t = 1) \Pr(S_t = j) + \\ &= (1 - \Pr(V_t = 1)) \Pr(S_{a,t} = j_a) \Pr(S_{b,t} = j_b), \end{aligned} \quad (15)$$

which implies that the joint dynamics of $S_{a,t}$ and $S_{b,t}$ remain characterized by a weighted average between the extreme dependent and independent cases, where the weights assigned to each of them are endogenously determined by

$$\Pr(V_t = 1) = \delta_t^{ab}. \quad (16)$$

Therefore, the term δ_t^{ab} from now on will be referred as the dynamic synchronicity between $S_{a,t}$ and $S_{b,t}$.

2.1 Filtering Algorithm

This section develops an extension of the Hamilton's (1994) algorithm to estimate the model described in Equations (4) and (15). The algorithm is composed by two unified steps, in the first one the goal is the computation of the likelihoods, while in the second one, to compute the prediction and updating probabilities.

STEP 1: The parameters of the model are assumed to be known for the moment and collected in the vector

$$\theta = (\mu_{a,0}, \mu_{a,1}, \mu_{b,0}, \mu_{b,1}, \sigma_a^2, \sigma_b^2, \sigma_{ab}, p_{a,00}, p_{a,11}, p_{b,00}, p_{b,11}, p_{00}, p_{11}, p_{v,00}, p_{v,11})'. \quad (17)$$

The conditional joint density corresponding to the state variable that fully characterizes

the model's dynamics, $S_{ab,t}^*$, can be expressed as a function of its components,

$$f(y_t, S_{ab,t}^* = j_{ab}^* | \psi_{t-1}; \theta) = f(y_t, S_{a,t} = j_a, S_{b,t} = j_b, V_t = j_v | \psi_{t-1}; \theta), \quad (18)$$

which is the product of the density conditional on the realization of the set of regimes times the probability of occurrence of such realizations,

$$f(y_t, S_{a,t} = j_a, S_{b,t} = j_b, V_t = j_v | \psi_{t-1}; \theta) = f(y_t | S_{a,t} = j_a, S_{b,t} = j_b, V_t = j_v, \psi_{t-1}; \theta) \times \Pr(S_{a,t} = j_a, S_{b,t} = j_b, V_t = j_v | \psi_{t-1}; \theta). \quad (19)$$

The trivariate probability of $S_{a,t} = j_a$, $S_{b,t} = j_b$ and $V_t = j_v$ is obtained by using conditional probabilities,

$$\Pr(S_{a,t} = j_a, S_{b,t} = j_b, V_t = j_v | \psi_{t-1}; \theta) = \Pr(S_{a,t} = j_a, S_{b,t} = j_b | V_t = j_v, \psi_{t-1}; \theta) \times \Pr(V_t = j_v | \psi_{t-1}; \theta), \quad (20)$$

where the term $\Pr(S_{a,t} = j_a, S_{b,t} = j_b | V_t = j_v, \psi_{t-1}; \theta)$ is fully characterized with the results derived in Equations (13) - (14). Thus, Equation (20) remains a function of just $\Pr(S_{k,t} = j_k | \psi_{t-1}; \theta)$ for $k = a, b$, $\Pr(V_t = j_v | \psi_{t-1}; \theta)$ and $\Pr(S_t = j | \psi_{t-1}; \theta)$. The steady state or ergodic probabilities can be used as starting values to initialize the filter.

In order to make inferences on the evolution of single state variables, the marginal densities are obtained as

$$f(y_t, S_{a,t} = j_a | \psi_{t-1}; \theta) = \sum_{j_b=0}^1 \sum_{j_v=0}^1 f(y_t, S_{a,t} = j_a, S_{b,t} = j_b, V_t = j_v | \psi_{t-1}; \theta), \quad (21)$$

$$f(y_t, S_{b,t} = j_b | \psi_{t-1}; \theta) = \sum_{j_a=0}^1 \sum_{j_v=0}^1 f(y_t, S_{a,t} = j_a, S_{b,t} = j_b, V_t = j_v | \psi_{t-1}; \theta), \quad (22)$$

$$f(y_t, V_t = j_v | \psi_{t-1}; \theta) = \sum_{j_a=0}^1 \sum_{j_b=0}^1 f(y_t, S_{a,t} = j_a, S_{b,t} = j_b, V_t = j_v | \psi_{t-1}; \theta), \quad (23)$$

The marginal density associated the state variable S_t requires a special treatment. When it is assumed that the model's dynamics are governed by only one state variables, i.e. $S_{a,t} = S_{b,t} = S_t$, the density in Equation (18) collapses to $f^\dagger(y_t, S_t = j | \psi_{t-1}; \theta)$, where

$$f^\dagger(y_t, S_t = 0 | \psi_{t-1}; \theta) = f(y_t, S_{a,t} = 0, S_{b,t} = 0, V_t = 1 | \psi_{t-1}; \theta) \quad (24)$$

$$f^\dagger(y_t, S_t = 1 | \psi_{t-1}; \theta) = f(y_t, S_{a,t} = 1, S_{b,t} = 1, V_t = 1 | \psi_{t-1}; \theta). \quad (25)$$

Accordingly, the density of y_t conditional on the past observables is given by

$$f(y_t|\psi_{t-1};\theta) = \sum_{j_a=0}^1 \sum_{j_b=0}^1 \sum_{j_v=0}^1 f(y_t, S_{a,t} = j_a, S_{b,t} = j_b, V_t = j_v|\psi_{t-1};\theta), \quad (26)$$

and under the assumption that $S_{a,t} = S_{b,t} = S_t$, it is given by

$$f^\dagger(y_t|\psi_{t-1};\theta) = \sum_{j=0}^1 f^\dagger(y_t, S_t = j|\psi_{t-1};\theta) \quad (27)$$

STEP 2: Once y_t is observed at the end of time t , the prediction probabilities $\Pr(S_{k,t} = j_k|\psi_{t-1};\theta)$ for $k = a, b$, $\Pr(V_t = j_v|\psi_{t-1};\theta)$ and $\Pr(S_t = j|\psi_{t-1};\theta)$ can be updated

$$\Pr(S_{a,t} = j_a|\psi_t;\theta) = \frac{f(y_t, S_{a,t} = j_a|\psi_{t-1};\theta)}{f(y_t|\psi_{t-1};\theta)} \quad (28)$$

$$\Pr(S_{b,t} = j_b|\psi_t;\theta) = \frac{f(y_t, S_{b,t} = j_b|\psi_{t-1};\theta)}{f(y_t|\psi_{t-1};\theta)} \quad (29)$$

$$\Pr(V_t = l|\psi_t;\theta) = \frac{f(y_t, V_t = l|\psi_{t-1};\theta)}{f(y_t|\psi_{t-1};\theta)} \quad (30)$$

$$\Pr(S_t = j|\psi_t;\theta) = \frac{f^\dagger(y_t, S_t = j|\psi_{t-1};\theta)}{f^\dagger(y_t|\psi_{t-1};\theta)}. \quad (31)$$

Forecasts of the updated probabilities in Equations (28)-(31) are done by using the corresponding transition probabilities $p_{a,ij}, p_{b,ij}, p_{ij}, p_{v,ij}$, in the vector θ , for $S_{a,t}, S_{b,t}, S_t, V_t$, respectively.

$$\begin{aligned} \Pr(S_{k,t+1} = j_k|\psi_t;\theta) &= \sum_{i_k=0}^1 \Pr(S_{k,t+1} = j_k, S_{k,t} = i_k|\psi_t;\theta) \\ &= \sum_{i_k=0}^1 \Pr(S_{k,t+1} = j_k|S_{k,t} = i_k) \Pr(S_{k,t} = i_k|\psi_t;\theta), \text{ for } k = a, b. \end{aligned} \quad (32)$$

$$\begin{aligned} \Pr(V_{t+1} = j_v|\psi_t;\theta) &= \sum_{i_v=0}^1 \Pr(V_{t+1} = j_v, V_t = i_v|\psi_t;\theta) \\ &= \sum_{i_v=0}^1 \Pr(V_{t+1} = j_v|V_t = i_v) \Pr(V_t = i_v|\psi_t;\theta) \end{aligned} \quad (33)$$

$$\begin{aligned} \Pr(S_{t+1} = j|\psi_t;\theta) &= \sum_{i=0}^1 \Pr(S_{t+1} = j, S_t = i|\psi_t;\theta) \\ &= \sum_{i=0}^1 \Pr(S_{t+1} = j|S_t = i) \Pr(S_t = i|\psi_t;\theta). \end{aligned} \quad (34)$$

Finally the above forecasted probabilities are used to predict inferences on the realiza-

tions of $S_{ab,t+1}^*$, relying on Equation (20)

$$\begin{aligned} \Pr(S_{a,t+1} = j_a, S_{b,t+1} = j_b, V_{t+1} = j_v | \psi_t; \theta) &= \Pr(S_{a,t+1} = j_a, S_{b,t+1} = j_b | V_{t+1} = j_v, \psi_t; \theta) \times \\ \Pr(V_{t+1} = j_v | \psi_t; \theta), \end{aligned} \quad (35)$$

where Equation (35) remains a function of $\Pr(S_{k,t+1} = j_k | \psi_t; \theta)$ for $k = a, b$, $\Pr(V_{t+1} = j_v | \psi_t; \theta)$ and $\Pr(S_{t+1} = j | \psi_t; \theta)$.

By iterating these two steps for $t = 1, 2, \dots, T$, the algorithm provides simultaneous inferences on $S_{a,t}$, $S_{b,t}$ and their dynamic synchronicity δ_t^{ab} , defined in Equation (16).

Regarding the estimation of the parameters, notice that as the number of possible states increase, the likelihood function could be characterized by several local maxima causing strong convergence problems in performing maximum likelihood estimation, Boldin (1996). Hence, given the high number of combinations of states through which the likelihood is conditioned in Equation (26), the set of parameters θ along with the inferences on the state variables are estimated by using Bayesian methods. Specifically, I use a multivariate version of the approach in Kim and Nelson (1999), which applies Gibbs sampling procedures. The estimation method is explained in detail in the Appendix.

2.2 Simulation Study

In order to validate the reliability of the proposed approach to assess changes in the synchronization of business cycle phases, I rely on the use of Monte Carlo experiments. Each simulation consists of two steps. First, the generation of two stochastic processes subject to regime switching that experiment one or more sync changes. Second, by letting the econometrician just observe the generated data, but not the data generating process, the proposed filter in Section 2.1 along with the Gibbs sampler are applied to obtain estimates of the model's parameters, probabilities of recession for each economy, and more importantly the inferences on synchronization changes. Then it is addressed how well the parameter estimates and inferences match the real ones.³

Given a sample of size T , the data generating process consists on generating a first order Markovian process, $S_{a,t}$, with transition probability matrix

$$P_a^* = \begin{pmatrix} p_{a,00}^* & 1 - p_{a,11}^* \\ 1 - p_{a,00}^* & p_{a,11}^* \end{pmatrix} \quad (36)$$

and an error term, $e_{a,t}^I$, drawn from a $N(0, 1)$. Then, given a vector of means $[\mu_{a,0}^*, \mu_{a,1}^*]'$

³It is important to notice that the filter's performance is assessed by simulations, under the assumption that the model is correctly specified. An interesting extension in this line of research could be assessing such performance by relaxing this assumption.

and standard error σ_a^* , I generate a process $y_{a,t}^I$ as follows

$$y_{a,t}^I = \mu_{a,0}^* + \mu_{a,1}^* S_{a,t} + \sigma_a^* e_{a,t}^I, \quad (37)$$

and given a vector of means $[\mu_{b,0}^*, \mu_{b,1}^*]'$, standard error σ_b^* and transition probabilities $p_{b,00}^*$ and $p_{b,11}^*$, the same procedure is repeated to independently generate

$$y_{b,t}^I = \mu_{b,0}^* + \mu_{b,1}^* S_{b,t} + \sigma_b^* e_{b,t}^I, \quad (38)$$

where $S_{b,t}$ is a first order Markovian process and $e_{b,t}^I$ is drawn from a $N(0, 1)$. Next, another Markovian process, S_t , is generated by using the transition matrix

$$P_{ab}^* = \begin{pmatrix} p_{00}^* & 1 - p_{11}^* \\ 1 - p_{00}^* & p_{11}^* \end{pmatrix}, \quad (39)$$

and an error term vector $[e_{a,t}^D, e_{b,t}^D]'$ is drawn from a bivariate normal distribution. Then, given the two vectors of means $[\mu_{a,0}^*, \mu_{a,1}^*]'$, $[\mu_{b,0}^*, \mu_{b,1}^*]'$, standard errors σ_a^* , σ_b^* , and a parameter σ_{ab}^* , I generate

$$\begin{bmatrix} y_{a,t}^D \\ y_{b,t}^D \end{bmatrix} = \begin{bmatrix} \mu_{a,0}^* + \mu_{a,1}^* S_t \\ \mu_{b,0}^* + \mu_{b,1}^* S_t \end{bmatrix} + \begin{bmatrix} \sigma_a^* & \sigma_{ab}^* \\ \sigma_{ab}^* & \sigma_b^* \end{bmatrix} \begin{bmatrix} e_{a,t}^D \\ e_{b,t}^D \end{bmatrix} \quad (40)$$

The information generated so far can be collected in two vectors, one in which two stochastic processes are driven by two Markov-switching variables independent from each other, $y_t^I = [y_{a,t}^I, y_{b,t}^I]'$, and the other where two stochastic processes are governed by only one Markov-switching dynamics, $y_t^D = [y_{a,t}^D, y_{b,t}^D]'$.

The premise in this paper claims that during some regimes, the output growth of two economies can follow dynamics similar to those in y_t^D , while during other regimes, things can change in one, or both, of the economies, leading their joint dynamics to behave as the ones in y_t^I , following independent patterns. To mimic this situation, I start analyzing the simplest case in which there is just one sync change in a sample of size T , occurred at time τ , with $1 < \tau < T$.⁴ Then, let $y_t = [y_{a,t}, y_{b,t}]'$ be the observed output growth of two economies, which come from the following unobserved data generating process:

$$y_t = \begin{cases} y_t^D, & \text{for } t = 1, \dots, \tau \\ y_t^I, & \text{for } t = \tau + 1, \dots, T \end{cases}, \quad (41)$$

⁴The selection of τ , is based on a random draw u , generated from a uniform distribution $U[0, 1]$, i.e. $\hat{\tau} = uT$, then $\hat{\tau}$ is rounded to the nearest integer number to obtain τ . Also, it is avoided the use of draws of τ equal to the boundaries, i.e. 1 or T .

that can be alternatively expressed as

$$y_t = y_t^D V_t + (1 - V_t) y_t^I, \quad (42)$$

where V_t is an indicator variable of synchronization, which dynamics are described by

$$\{V_t\}_1^T = \begin{bmatrix} \mathbf{1}_\tau \\ \mathbf{0}_{T-\tau} \end{bmatrix}, \quad (43)$$

with $\mathbf{1}_\tau$ being a vector of ones of size τ and $\mathbf{0}_{T-\tau}$ a zero vector of size $T - \tau$. The case of one sync change can be easily extended to mimic the case of Z sync changes, occurred at $\tau_1, \tau_2, \dots, \tau_Z$, with $1 < \tau_1 < \tau_2 < \dots < \tau_Z < T$, just by appropriately modifying the dynamics in $\{V_t\}_1^T$.

Since the data generating process and parameters are unknown by the econometrician, the Gibbs sampler is used to estimate the model's parameters, the probabilities of recession for each economy, and more importantly inferences on the dynamics of V_t , by relying on the filtering algorithm proposed in Section 2.1. The criterion used to assess the performance of the regime inferences and the synchronization is the Quadratic Probability Score (QPS) defined as

$$QPS(\Xi) = \frac{1}{T} \sum_{t=1}^T (\Xi - \Pr(\Xi = 1 | \psi_T))^2, \text{ for } \Xi = S_{a,t}, S_{b,t}, V_t. \quad (44)$$

To illustrate the filtering and estimation strategy's performance, Figure 1 plots one simulation for the cases in which there is one, two and three sync changes in a sample of 200 periods, i.e. for $z = 1, 2, 3$, with $T = 200$. For each case, the top charts plot the two observed time series, $y_{a,t}$ and $y_{b,t}$, generated with the parameter values in Table 1 and by using Equation (42), along with the unobserved dynamics of V_t . Both time series show strong coherence in phases when $V_t = 1$, and the opposite occurs while $V_t = 0$. The two middle charts plot the probabilities of recession associated to each time series, i.e. $\Pr(S_{k,t} = 0 | \psi_T)$, for $k = a, b$, showing values near to one when the corresponding time series reports consecutive negative values, also the dynamics of V_t is plotted as reference. Finally, the bottom charts plot the computed inferences on the synchronization changes, i.e. $\Pr(V_t = 1)$, along with the true dynamics of V_t , showing their close relation in all the three cases and giving insights about the satisfactory performance of the proposed framework in assessing synchronization changes.

This experiment is replicated $M = 1000$ times for $Z = 6$ different cases. Each case corresponds to z changes in sync, for $z = 1, 2, 3, 4, 5$, and the last case considers a random number of sync changes, i.e. unlike predefining the dynamics of V_t as in Equation (43), it is modeled as a first order Markov chain with transition probabilities $p_{V,00}^*$ and $p_{V,11}^*$, i.e.

$z = f(V_t)$.⁵

The result of the Monte Carlo simulations are reported in Table 2, showing the average over the M replications of each estimated parameter

$$\theta_z^* = \frac{1}{M} \sum_{m=1}^M \theta_z^{*(m)}, \quad (45)$$

where $\theta_z^{*(m)}$ corresponds to the vector of parameters, as defined in Equation (17), associated to the m -th replica and the z -th case. All parameter estimates appear to be unbiased for the different values of z . Although, two features deserve attention. First, the stochastic process with the highest difference of the within-regime means, in this case $y_{b,t}$, shows more accurate estimates, meaning that higher differences provide a better identification of the phases of the business cycles.⁶ Second, the accuracy in the estimation of the transition probabilities decreases when $z = f(V_t)$, this is due to the high number of sync changes and the short duration of each change generated by letting V_t to follow Markovian dynamics.

Regarding the performance about the regime inferences, Table 3 reports the averages over the M replications of the QPS associated to the state variables $S_{a,t}$, $S_{b,t}$ and V_t , which can be interpreted as the average over the M replications of the squared deviation from the generated business cycles.

$$QPS(\Xi)_z = \frac{1}{M} \sum_{m=1}^M QPS(\Xi)_z^{(m)}, \text{ for } \Xi = S_{a,t}, S_{b,t}, V_t \quad (46)$$

where $QPS(\Xi)_z^{(m)}$, as defined in Equation (44), corresponds to the m -th replica and the z -th case. The results indicate that, although inferences on the state variables in general present high precision, the ones associated to the time series with highest difference of the within-regime means, $y_{b,t}$, are the most accurate. The main message of the table is that precision of the inferences decreases as the number of sync changes, k , increases. This feature can also be observed by looking at the histograms of the M replications plotted in Figure 2, in particular the ones associated to $QPS(V_t)$. However, it is natural to think on synchronization changes as events that do not occur as often as the business cycle phases of an economy, but that require longer periods of time to take place, since they are originated from changes in the structural relationships among economies, letting the proposed model be suitable to accurately infer sync changes of business cycle phases.

⁵This is done using the corresponding values given in Table 1.

⁶The parameters associated to the variance-covariance matrix of y_t are not analyzed in Table 2 due to such matrix changes through the regimes of dependence and therefore are not comparable with the estimated ones.

3 Monitoring U.S. States Business Cycles Synchronization

The last global financial crisis has stimulated the interest in the study of the sources and propagation of contractionary episodes, calling to take a more careful look at the disaggregation of the business cycle in order to assess the mechanisms underlying economic fluctuations. On the one hand, recent work by Acemoglu et al. (2012) that relies on network analysis, finds that sectoral interconnections capture the possibility of “cascade effects” whereby productivity shocks to a sector propagate not only to its immediate downstream customers, but also to the rest of the economy.

On the other hand, two recent works have shown interesting features of economic activity phases synchronization when the business cycle is disaggregated at the regional level. In the first one, Owyang et al. (2005) investigate the evolution of the individual business cycle phases of the U.S. states. By following a univariate approach, the authors find that U.S. states differ significantly in the timing of switches between regimes of expansions and recessions, and also differ in the extent to which state business cycle phases are in concord with those of the national economy. In the second one, Hamilton and Owyang (2012) use a unified framework to go through the propagation of regional recessions in U.S., using a multivariate approach that focuses on clustering the states sharing similar business cycle characteristics, finding that differences across states appear to be a matter of timing and that they can be grouped into three clusters, with some of them entering recession or recovering before others. Although these previous studies provide useful insights about the overall synchronization pattern in given sample period, they are not able to detect changes in such patterns occurred during such time span.

The present application intends to unify both concepts, dynamic synchronization of pairwise cycles, by using the framework proposed in Section 2, and the dynamic interdependence between all U.S. states, by relying on network analysis, in order to assess the presence and the nature of potential changes in the regional propagation of contractionary shocks. For this purpose I use data on U.S. states coincident indexes, proposed in Crone (2002) and provided by the Federal Reserve Bank of Philadelphia, as monthly indicators of the overall economic activity at the state level for the time span 1979:08 - 2013:03, Alaska and Hawaii are excluded as in Hamilton and Owyang (2012). The Chicago Fed National Activity Index (CFNAI) is used as monthly measure of the U.S. national business cycle. All these indexes of real economic activity, for each states and for U.S., have been constructed by the corresponding authors based on the principle of comovement among industrial production, employment, sales, and income measures.

3.1 Bivariate Analysis

The analysis for 48 U.S. states plus U.S. as a whole requires to model each of the $C_2^{49} = 1176$ pairwise comparisons. To assess the performance of the proposed Markov-switching synchronization model, two selected examples are analyzed in detail.⁷ The first example focuses on the case of two states that present high share of national GDP, New York with 7.68% and Texas with 7.95%. Table 4 reports the Bayesian estimates for the *New York vs. Texas* model, showing negative growth rates when $S_t = 0$ and positive growth when $S_t = 1$, for both states. It is worth to highlight the estimates of the transition probabilities associated to the state variable that measures synchronization, V_t . The probability of remaining in a regime of high synchronization is almost equal to the probability of remaining in a low sync regime, about 0.96. This result is corroborated in Chart A of Figure 3, which plots the probabilities of recession for New York and Texas along with the corresponding time-varying synchronization, $\delta_t^{NY, TX}$, as defined in Equation (16). As can be in the top and middle charts, since the eighties until the mid-nineties these states were experimenting recessions with different timing, this is reflected in the low values of the synchronicity, plotted at the bottom of chart A. However, after the mid-nineties until the present time, both economies have been experiencing the same recession's chronology, which is consistent with the increase in the synchronicity observed after the mid-nineties.

The second example analyzes the case of two states with different GDP shares, the state with the highest one, California with 13.34%, and the state with the lowest one, Vermont with 0.18%. Table 5 presents the Bayesian parameter estimates of the model. Unlike to the previous example, in the *California vs. Vermont* model, the probability of remaining in a high sync regime, 0.97, is higher than the probability of remaining in a low sync regime, 0.93. This agrees with Chart B of Figure 3, which shows that in general both states have been experiencing the same business cycle chronology, entering recessions and expansions synchronously, with the exception of some period. In 1989 Vermont entered in a recessionary phase, while California was still growing, until the mid-1990, when it started to experience a recession. However, at the beginning of 1992, Vermont started an expansionary phase, while California continued in recession until 1994. These desynchronicities are reflected in the downturn of the time-varying sync, $\delta_t^{CA, VT}$, during that period, shown at the bottom panel of Chart B.

All the remaining pairwise cases were also estimated, although the results are not shown to save space, they are available upon request to the author. Considerable heterogeneity was found in the dynamics of the estimated time-varying synchronizations, finding cases involving significant changes, and cases where the synchronization was almost constant, at low or high levels. Despite the proposed framework is able to provide information on the synchronization between any pair of states for any given period of time, when policy

⁷The results for the other 1,126 cases are available upon request to the author.

makers are interested in the "big picture" of the overall regional synchronization path, other ways of summarize the information are needed.

3.2 Multivariate Analysis

As suggested by Timm (2002) and Camacho et al. (2006), multidimensional scaling (MDS) method is a helpful tool to identify cyclical affiliations between economies, since it seeks to find a low dimensional coordinate system to represent n -dimensional objects and create a map of lower dimension (k). Traditionally, studies use as input for this method a symmetric matrix, Γ , that summarizes the cyclical distances between economies for a given time span, each entry γ^{ij} of the matrix assigns a value characterizing the distance between economies i and j . The output of the MDS consists on one map showing the general picture for all the cyclical affiliations.

The dynamic synchronization measures obtained in the bivariate analysis, $0 \leq \delta_t^{ij} \leq 1$, can be easily converted into desynchronization measures, $\gamma_t^{ij} = 1 - \delta_t^{ij}$. Accordingly, γ_t^{ij} can be interpreted as cyclical distances allowing the construction of the dissimilarity matrix Γ , for each time period

$$\Gamma_t = \begin{pmatrix} 1 & \gamma_t^{12} & \gamma_t^{13} & \dots & \gamma_t^{1n} \\ \gamma_t^{21} & 1 & \gamma_t^{23} & \dots & \gamma_t^{2n} \\ \gamma_t^{31} & \gamma_t^{32} & 1 & \dots & \gamma_t^{3n} \\ \vdots & \vdots & \vdots & \ddots & \vdots \\ \gamma_t^{n1} & \gamma_t^{n2} & \gamma_t^{n3} & \dots & 1 \end{pmatrix}, \quad (47)$$

providing the possibility of assessing changes in the general picture of all cyclical affiliations of U.S. states.

In a recent work on MDS, Xu et al. (2012) proposed a way to deal with MDS in a dynamic fashion, where the dimensional coordinates of the projection of any two objects, i and j , are computed by minimizing the stress function

$$\min_{\tilde{\gamma}_t^{ij}} = \frac{\sum_{i=1}^n \sum_{j=1}^n (\gamma_t^{ij} - \tilde{\gamma}_t^{ij})^2}{\sum_{i,i} (\gamma_t^{ij})^2} + \beta \sum_{i=1}^n \tilde{\gamma}_{t|t-1}^i, \quad (48)$$

where

$$\tilde{\gamma}_t^{ij} = (\|z_{i,t} - z_{j,t}\|^2)^{1/2} \quad (49)$$

$$\tilde{\gamma}_{t|t-1}^i = (\|z_{i,t} - z_{i,t-1}\|^2)^{1/2}, \quad (50)$$

being $z_{i,t}$ and $z_{j,t}$ the k -dimensional projection of the objects i and j , and β a temporal regularization parameter that serves to zoom in or zoom out changes between frames at t

and at $t + 1$, keeping always the same dynamics independently on its value. In principle it can be simply set up to 1, however since the data in Γ_t belong to the unit interval, for a more adequate visual perception of the transitions between frames it is set up to 0.1. The output of the minimization in Equation (48) provides a bidimensional representation of Γ_t .

The synchronization maps of U.S. states for the first month of the last four recessions are plotted in the charts of Figure 4. Each point in the charts represents a states, the middle point refers to U.S. nation as a whole. The closeness between two points in the plane makes reference to their synchronicity degree, i.e. the closer are the points, the higher is their synchronization. The figure corroborates the premise in the introduction of this paper about the existence of significant changes in the grouping pattern among regional economies through time. Specifically, the top-left chart plots the scenario for the 1981's recession, where a big group of states were in synchronized with each other, while the remaining states, such as Florida, Colorado, Texas, North Dakota, West Virginia, among others, were following independent patterns. Also, notice that states such as Nevada, North Carolina, Vermont, Tennessee, were the ones more in sync with the U.S. business cycle during that month. The top-right corner presents the situation for the 1990's recession, showing a different grouping pattern characterized by one big group of states in sync with each other and two small clusters, the first one composed by New Hampshire, Massachusetts, Connecticut, Vermont, New Jersey, Maine and Rhode Island, and the second one by New York, Virginia, Delaware and Maryland. Notice that in this month, states such as Florida, Pennsylvania, California, among others, were the ones more in sync with the U.S. cycle. The bottom charts present the scenarios for the 2001's and 2007's recessions, in the left and right corner respectively. Again, the pattern changed with respect to the previous episodes, since the last two recessions were characterized by a core (composed by states highly in sync) and periphery (composed by independent states) structure, finding the core of the later one tighter than the in the former. The full animated representation can be found at the author's web page.⁸

An additional advantage of the proposed framework is the possibility of recovering the stationary measures of synchronization, by using the ergodic probabilities associated to the latent variable V_t . Chart A of Figure 5 plots the stationary grouping pattern, which can be interpreted as the *average* pattern during 1979:08 - 2013:03, showing three groups of states, one of them is closer to the U.S. cycle, the second one is less but still close to the U.S. cycle, while the third one is characterized by the states following independent dynamics. To assess if this result reconciles the one in Hamilton and Owyang (2012), Chart B of Figure 5 plots the clusters obtained by those authors, clearly finding that both results coincide, not just in the number of clusters but also in the states that correspond

⁸<https://sites.google.com/site/daniloleivaleon/media>

to each cluster. Moreover, this result is not only robust to the methodology employed, but also to the data used, since Hamilton and Owyang (2012) used annualized quarter-to-quarter growth rates of payroll employment, while I use monthly growth rates of state coincident indexes of economic activity. These facts show one of the main contributions of the proposed framework, which is provide synchronization measures that may change over time, and moreover can be collapsed into ergodic measures that yield results consistent with the ones in previous work.

Regarding the cyclical relationship between states and the national business cycle, Table 6 reports the corresponding ergodic synchronizations, showing that it ranges from the highest, which is North Carolina with 0.91, until the lowest one, which corresponds to Oklahoma with 0.19, revealing that states with the highest GDP share do not necessarily represent the states showing the highest synchronicity with the national business cycle. To provide a visual perspective, Chart A of Figure 6 plots a U.S. map with the estimates obtained in this paper and Chart B, of the same figure, plots the concordance pattern obtained in Owyang et al. (2005) by calculating the percentage of the time two economies were in the same regime based on univariate MS models for each state. Although both results report high values in most of the states located in the east region and medium values in few states located in the west, the stationary sync measure presents higher dispersion than the concordance, as can be seen in the associated histograms, helping to disentangle in a more precise way the cyclical relationship between states and the nation.

3.3 Network Analysis

In recent works by Carvalho (2008), Gabaix (2011), Acemoglu et al. (2012), among others, it is shown how idiosyncratic shocks, at the firm or sectoral level, may originate macroeconomic fluctuations given their interlinkages by relying on network analysis. Although, such analysis primarily relies on the economy’s sectoral disaggregation, it turns out interesting to assess if another type of disaggregation, e.g. regional, may also have significant implications on aggregate fluctuations.

The intuition behind the synchronization measure in Equation (16) relies on the fact that if δ_t^{ij} is close to 1, it is likely that at time t , economies i and j are sharing the same business cycle phases, creating a link of interdependence between them. On the other hand, if δ_t^{ij} is close to 0, it means that they are following independent phases and hence are not linked.⁹ Therefore, by letting $H = \{h_i\}_1^n$ be the set of n economies taking the interpretation of nodes, h_i for $i = 1, \dots, n$, and defining δ_t^{ij} as the probability that nodes h_i and h_j are linked at time t , the matrix $\Delta_t = \mathbf{1}_n - \Gamma_t$, can be interpreted as

⁹Notice that the proposed synchronization modeling approach distinguishes between the state in which two economies are in recession because their cycles are independent, and they just coincided, from the state where the two economies are in recession because they are under a regime of dependence, i.e. states 1 and 5 of $S_{ab,t}^*$ in Equation (11), respectively.

a weighted network of synchronization with Markovian dynamics.¹⁰ Consequently, the cyclical interdependence of a large set of economies can be dynamically assessed under a unified framework by relying on network analysis. It is worth to notice that although the construction of Δ_t requires the computation several bivariate models of the type in Equation (4), it may be less restrictive and involve less parameter and regime's uncertainty than the computation of a framework with similar nonlinear nature but involving all n economies simultaneously, however further research in this respect would be desired.

To provide a glimpse of the shape that the Markov-switching synchronization network (MSYN) have taken during contractionary episodes, the charts of Figure 7 plot the corresponding network graph for the first month of the last four recessions. Given that the MSYN is a weighted network, in order to make possible the graphical representation, a link between nodes i and j is plotted if $\delta_t^{ij} > 0.5$, otherwise no link is plotted between them. The figure corroborates the grouping pattern of one big cluster and independent states in the 1981's recession, some small clusters in the 1990's recession and a core and periphery structure and the 2001's and 2007's recessions, with a more concentrated core in the last recession.¹¹

The main advantage of providing a network analysis for the present framework is that all the information on synchronicities so far studied can be summarized in just one measure, the closeness centrality. There are several measures regarding the centrality of a network, but given that desynchronization measures are interpreted as distances, the most appropriate one for this context is the closeness.

Two variations of the closeness centrality are analyzed in this section for robustness purposes. For each of them, it is necessary first to compute the centrality of each node

$$C_t(i) = \frac{1}{\sum_{j \neq i|t} d_t(i, j)}, \text{ for } i = 1, 2, \dots, n, \quad (51)$$

where $d(i, j)$ is the length of the shortest path between nodes i and j , which can be computed by the Dijkstra's (1959) algorithm.¹² Thus, the more central is a node, the lower is its total distance to all other nodes. Closeness can be regarded as a measure of how fast it will take to spread information, e.g. risk, economic shocks, etc., from node i to all other nodes sequentially. For an overview regarding to definitions in network analysis, see Goyal (2007).

Once the dynamic centrality of each node has been computed, the information about

¹⁰The term $\mathbf{1}_n$ represents a squared matrix of size n with all entries equal to 1.

¹¹Notice that although the U.S. business cycle is not included in the network analysis, just the ones of the states, each chart in the figure shows a close relation with the corresponding one in Figure 4

¹²For example, in a set $H' = \{a, b, c\}$ where the distances $\gamma = 1 - \delta$, are given by $\gamma^{ab} = 0.5$, $\gamma^{ac} = 0.9$ and $\gamma^{bc} = 0.2$, the shortest path between a and c will be 0.7, since $\gamma^{ab} + \gamma^{bc} < \gamma^{ac}$. Thus, notice that $d(a, c)$ does not necessarily have to be equal to γ^{ac} .

the whole network’s centrality typically can be assessed as follows

$$C_t^N = \sum_{i=1|t}^k [C_t(i^*) - C_t(i)], \quad (52)$$

where i^* is the node that attains the highest closeness centrality across all nodes at time t . The second measure, consists on the average across all nodes’ centralities, $C_t(i)$, defined by

$$C_t^A = \sum_{i=1|t}^k C_t(i). \quad (53)$$

These two measures that provide information on the changes in the degree of aggregate synchronization among the economies in the set H , for the present case between the states of U.S., can be used to investigate the relationship between regional business cycle interdependence and the aggregate fluctuations.¹³

One of the main findings in Hamilton and Owyang (2012) is the substantial heterogeneity across regional recessions in U.S. at the state level. However, how could such heterogeneity change over time? is an issue that has remained not investigated. The proposed framework is used to dynamically quantify the substantial regional heterogeneity under the unified setting MSYN. The intuition behind the state’s centrality in Equation (51) is the following: if at time t , state i is highly synchronized with respect to the rest of U.S. states its total distance to them, $\sum_{j \neq i|t} d_t(i, j)$, would tend to be low and its centrality, $C_t(i)$, to be high. If a similar behavior occurs with the remaining $n - 1$ states, the MSYN’s centrality would also tend to take high values. Meaning that, high global interdependence, or equivalently, high homogeneity of regional recessions, is associated to high values of the MSYN’s centrality C_t^Υ , for $\Upsilon = N, A$.

The Chart A of Figure 8 plots the network centrality, C_t^N , and the average centrality, C_t^A , in standardized terms to facilitate their comparison. Both measures show similar dynamics, experimenting substantial changes over time which have a close relation with the national recessions dated by the NBER, and showing some interesting features. First, the centrality shows a markedly high tendency to increase some months before national recessions take place, keeping high values during the whole contractionary episode, implying that sudden increases in the degree of interdependence among states may be useful to signal upcoming national recessions.

Second, once national recessions have ended, the centrality still remains high during some period of time. This is because the whole economy is recovering from the recession and most of the states are synchronized, but this time in an recovery regime. Notice that

¹³A third measure based on extracting the common component among the nodes’ centralities by using principal component analysis was also computed. However, the results were similar to the ones of obtained with the average centrality. Therefore, they are not shown.

the highest interdependence level, occurred in October 2003, roughly coinciding with the highest growth rate of real GDP experienced by the U.S. economy since the end of 2000 up to the present time.

Third, after this phase of recovery has ended and the U.S. economy starts its moderated expansionary path, the centrality decreases until it reaches a certain stable level, which prevails until another recession takes place and the cycle repeats. Notice that the periods with higher heterogeneity across regional business cycles do not occur during recessions or recoveries, but during periods of stable economic expansion. These three observations reveal that regional economies in U.S. at the state level are subject to cycles of interdependence which are highly associated to the national business cycle.

Fourth, the centrality measures during the last two national recessions were almost twice higher than during the previous ones, corroborating the core-periphery structure observed in the MDS analysis for the corresponding periods and plotted in the bottom charts of Figure 7. This result discloses a change in the propagation pattern of aggregate recessionary shocks. On the one hand, during the pre-2000's recessions those shocks were spread mainly toward few but big states, in terms of GDP share, such as California, Georgia, Massachusetts, New Jersey and New York during the 1981's recession, and such as Florida, Georgia, North Carolina and Pennsylvania during the 1990's recession. On the other hand, during the post-2000's recessions such shocks were more uniformly and synchronously distributed across states, in particular to the ones in the core which were the majority, as can be seen in the charts of Figure 4. For robustness purposes the centrality measures were also computed but using the filtered, instead of the smoothed, probabilities of V_t which are plotted in Chart B of Figure 8, finding essentially the same results.

Finally, to address changes in the clustering pattern in a statistical rather than visual manner, I compute the clustering coefficient of the MSYN, for every period of time by following Strogatz and Watts (1998), which allows to measure the level of cohesiveness between the business cycle phases of U.S. states. The dynamic clustering coefficient is plotted in Figure 9, showing relatively low values during the 1980, 1981 and 1990's recessions and high values during the 2001 and 2007's recessions. Moreover, it shows that in the mid 90's there was a significant change in the regional cohesiveness, since before that time, the clustering coefficient behaved following short cycles, but after that, it remained almost stable at higher values, corroborating the change in the propagation of contractionary shocks occurred since the 2000's recession and providing evidence that U.S. economy's regions have become more interdependent since the early 90s.

There are several potential channels driving this change, such as macroeconomic or financial factors, however these issues remain pending for further research in this line.

4 Conclusions

Most of the studies on business cycle synchronization provide a general pattern of cyclical affiliations between economies for a given time span. However, few has been done in assessing potential changes in that pattern occurred during such time span. This paper proposed an extended Markov-switching framework to assess changes in the synchronization of cycles by inferring the time-varying dependency relationship between the latent variables governing Markov-switching models. The reliability of the approach to track sync changes is confirmed by Monte Carlo experiments.

The proposed framework is applied to investigate potential variations in the cyclical interdependence between the states of U.S., obtaining three main findings. First, the results report the existence of interdependence cycles which are associated to NBER recessions, such cycles are defined as periods characterized by low cyclical heterogeneity across states, experienced during the recessionary and recovery phases, followed by longer periods of high cyclical heterogeneity, occurred during the phases of stable growth. Second, there are substantial variations in the grouping pattern of states over time that can be monitored on a monthly basis, going from a scheme characterized by several clusters of states to a core and periphery structure, composed by highly and lowly synchronized states, respectively. Third, there is evidence of a change in the propagation pattern of recessionary shocks across states, which were spread mainly toward few but big states, in terms of GDP share, until the 1991's recession, but after that, contractionary shocks were more synchronously and uniformly spread toward most of the U.S. states, implying that U.S. economy's regions have become more interdependent since the early 90s.

Appendix

A Bayesian Parameter Estimation

The approach to estimate θ will be relied on a bivariate extended version of the multi-move Gibbs-sampling procedure implemented by Kim and Nelson (1998) for Bayesian estimation of univariate Markov-switching models. In this setting both the parameters of the model θ and the Markov-switching variables $\tilde{S}_{k,T} = \{S_{k,t}\}_1^T$ for $k = a, b$, $\tilde{S}_T = \{S_t\}_1^T$ and $\tilde{V}_T = \{V_t\}_1^T$ are treated as random variables given the data in $\tilde{y}_T = \{y_t\}_1^T$. The purpose of this Markov chain Monte Carlo simulation method is to approximate the joint and marginal distributions of these random variables by sampling from conditional distributions.

A.1 Priors

For the mean and variance parameters in vector θ , the Independent Normal-Wishart prior distribution is used

$$p(\mu, \Sigma^{-1}) = p(\mu)p(\Sigma^{-1}), \quad (54)$$

where

$$\begin{aligned} \mu &\sim N(\underline{\mu}, \underline{V}_\mu) \\ \Sigma^{-1} &\sim W(\underline{S}^{-1}, \underline{v}), \end{aligned}$$

and the associated hyperparameters are given by $\underline{\mu} = (-1, 2 - 1, 2)'$, $\underline{V}_\mu = I$, $\underline{S}^{-1} = I$, $\underline{v} = 0$.

For the transition probabilities $p_{a,00}, p_{a,11}$ from $S_{a,t}$, $p_{b,00}, p_{b,11}$ from $S_{b,t}$, p_{00}, p_{11} from S_t and $p_{v,00}, p_{v,11}$ from V_t , Beta distributions are used as conjugate priors

$$p_{k,00} \sim Be(u_{k,11}, u_{k,10}), p_{k,11} \sim Be(u_{k,00}, u_{k,01}), \text{ for } k = a, b \quad (55)$$

$$p_{v,00} \sim Be(u_{v,11}, u_{v,10}), p_{v,11} \sim Be(u_{v,00}, u_{v,01}), \quad (56)$$

$$p_{00} \sim Be(u_{11}, u_{10}), p_{11} \sim Be(u_{00}, u_{01}) \quad (57)$$

where the hyperparameters are given by $u_{\iota,01} = 2$, $u_{\iota,00} = 8$, $u_{\iota,10} = 1$ and $u_{\iota,11} = 9$, for $\iota = a, b, v, _$. For each pairwise model, 6000 iterations were performed, discarding the first 1000.

A.2 Drawing $\tilde{S}_{a,T}, \tilde{S}_{b,T}, \tilde{S}_T$ and \tilde{V}_T given θ and \tilde{y}_T

Following the result in Equation (15), in order to make inference on the bivariate dynamics of the model (4) driven by $\tilde{S}_{ab,T} = \{S_{ab,t}\}_1^T$ and described in (6), it is just needed to make

inference on the dynamics of the single state variables $\tilde{S}_{a,T}$, $\tilde{S}_{b,T}$, \tilde{S}_T and \tilde{V}_T , this can be done following the results in Kim and Nelson (1998) by first computing draws from the conditional distributions

$$g(\tilde{S}_{k,T}|\theta, \tilde{y}_T) = g(S_{k,T}|\tilde{y}_T) \prod_{t=1}^T g(S_{k,t}|S_{k,t+1}, \tilde{y}_t), \text{ for } k = a, b \quad (58)$$

$$g(\tilde{S}_T|\theta, \tilde{y}_T) = g(S_T|\tilde{y}_T) \prod_{t=1}^T g(S_t|S_{t+1}, \tilde{y}_t) \quad (59)$$

$$g(\tilde{V}_T|\theta, \tilde{y}_T) = g(V_T|\tilde{y}_T) \prod_{t=1}^T g(V_t|V_{t+1}, \tilde{y}_t). \quad (60)$$

In order to obtain the two terms in the right hand side of Equation (58)-(59) the following two steps can be employed:

Step 1: The first term can be obtained by running the filtering algorithm developed in Section 2.1, to compute $g(\tilde{S}_{k,t}|\tilde{y}_t)$ for $k = a, b$, $g(\tilde{S}_t|\tilde{y}_t)$ and $g(\tilde{V}_{k,t}|\tilde{y}_t)$ for $t = 1, 2, \dots, T$, saving them and taking the elements for which $t = T$.

Step 2: The product in the second term can be obtained for $t = T - 1, T - 2, \dots, 1$, by following the result:

$$\begin{aligned} g(S_t|\tilde{y}_t, S_{t+1}) &= \frac{g(S_t, S_{t+1}|\tilde{y}_t)}{g(S_{t+1}|\tilde{y}_t)} \\ &\propto g(S_{t+1}|S_t)g(S_t|\tilde{y}_t), \end{aligned} \quad (61)$$

where $g(S_{t+1}|S_t)$ corresponds to the transition probabilities of S_t and $g(S_t|\tilde{y}_t)$ were saved in Step 1.

Then, it is possible to compute

$$\Pr[S_t = 1|S_{t+1}, \tilde{y}_t] = \frac{g(S_{t+1}|S_t = 1)g(S_t = 1|\tilde{y}_t)}{\sum_{j=0}^1 g(S_{t+1}|S_t = j)g(S_t = j|\tilde{y}_t)}, \quad (62)$$

and generate a random number from a $U[0, 1]$. If that number is less than or equal to $\Pr[S_t = 1|S_{t+1}, \tilde{y}_t]$, then $S_t = 1$, otherwise $S_t = 0$. The same procedure applies for $S_{a,t}$, $S_{b,t}$ and V_t , and by using Equation (15) inference of $\tilde{S}_{ab,T}$ can be done.

A.3 Drawing $p_{a,00}, p_{a,11}, p_{b,00}, p_{b,11}$, $p_{00}, p_{11}, p_{v,00}, p_{v,11}$ given $\tilde{S}_{a,T}, \tilde{S}_{b,T}, \tilde{S}_T$ and \tilde{V}_T

Conditional on $\tilde{S}_{k,T}$ for $k = a, b$, \tilde{S}_T and \tilde{V}_T , the transition probabilities are independent on the data set and the model's parameters. Hence, focusing on the case of \tilde{S}_T , the likelihood function of p_{00} , p_{11} is given by:

$$L(p_{00}, p_{11}|\tilde{S}_T) = p_{00}^{n_{00}}(1 - p_{00}^{n_{01}})p_{11}^{n_{11}}(1 - p_{11}^{n_{10}}), \quad (63)$$

where n_{ij} refers to the transitions from state i to j , accounted for in \tilde{S}_T .

Combining the prior distribution in Equation (57) with the likelihood, the posterior distribution is given by

$$p(p_{00}, p_{11} | \tilde{S}_T) \propto p_{00}^{u_{00} + n_{00} - 1} (1 - p_{00})^{u_{01} + n_{01} - 1} p_{11}^{u_{11} + n_{11} - 1} (1 - p_{11})^{u_{10} + n_{10} - 1} \quad (64)$$

which indicates that draws of the transition probabilities will be taken from

$$p_{00} | \tilde{S}_T \sim Be(u_{00} + n_{00}, u_{01} + n_{01}), \quad p_{11} | \tilde{S}_T \sim Be(u_{11} + n_{11}, u_{10} + n_{10}). \quad (65)$$

The same procedure applies for the cases of $\tilde{S}_{k,T}$ for $k = a, b$ and \tilde{V}_T .

A.4 Drawing $\mu_{0,a}, \mu_{1,a}, \mu_{0,b}, \mu_{1,b}$ given $\sigma_a^2, \sigma_b^2, \sigma_{ab}, \tilde{S}_{a,T}, \tilde{S}_{b,T}, \tilde{S}_T, \tilde{V}_T$ and \tilde{y}_T

The model in Equation (4) can be compactly expressed as

$$\begin{bmatrix} y_{a,t} \\ y_{b,t} \end{bmatrix} = \begin{bmatrix} 1 & S_{a,t} & 0 & 0 \\ 0 & 0 & 1 & S_{b,t} \end{bmatrix} \begin{bmatrix} \mu_{a,0} \\ \mu_{a,1} \\ \mu_{b,0} \\ \mu_{b,1} \end{bmatrix} + \begin{bmatrix} \varepsilon_{a,t} \\ \varepsilon_{b,t} \end{bmatrix}, \quad \begin{bmatrix} \varepsilon_{a,t} \\ \varepsilon_{b,t} \end{bmatrix} \sim N \left(\begin{bmatrix} 0 \\ 0 \end{bmatrix}, \begin{bmatrix} \sigma_a^2 & \sigma_{ab} \\ \sigma_{ab} & \sigma_b^2 \end{bmatrix} \right)$$

$$y_t = \tilde{S}_t \mu + \xi_t, \quad \xi_t \sim N(\mathbf{0}, \Sigma), \quad (66)$$

stacking as:

$$y = \begin{bmatrix} y_1 \\ y_2 \\ \vdots \\ y_T \end{bmatrix}, \quad \bar{S} = \begin{bmatrix} \bar{S}_1 \\ \bar{S}_2 \\ \vdots \\ \bar{S}_T \end{bmatrix}, \quad \text{and } \xi = \begin{bmatrix} \xi_1 \\ \xi_2 \\ \vdots \\ \xi_T \end{bmatrix},$$

the model in Equation (66) remains written as a normal linear regression model with an error covariance matrix of a particular form:

$$y = S\mu + \xi, \quad \xi \sim N(\mathbf{0}, I \otimes \Sigma) \quad (67)$$

Conditional on the covariance matrix parameters, state variables and the data, by using the corresponding likelihood function, the conditional posterior distribution

$p(\mu | \tilde{S}_{a,T}, \tilde{S}_{b,T}, \tilde{S}_T, \tilde{V}_T, \Sigma^{-1}, \tilde{y}_T)$ takes the form

$$\mu | \tilde{S}_{a,T}, \tilde{S}_{b,T}, \tilde{S}_T, \tilde{V}_T, \Sigma^{-1}, \tilde{y}_T \sim N(\bar{\mu}, \bar{V}_\mu), \quad (68)$$

where

$$\begin{aligned}\bar{V}_\mu &= \left(\underline{V}_\mu^{-1} + \sum_{t=1}^T \bar{S}_t' \Sigma^{-1} \bar{S}_t \right)^{-1} \\ \bar{\mu} &= \bar{V}_\mu \left(\underline{V}_\mu^{-1} \underline{\mu} + \sum_{t=1}^T \bar{S}_t' \Sigma^{-1} y_t \right).\end{aligned}$$

After drawing $\mu = (\mu_{a,0}, \mu_{a,1}, \mu_{b,0}, \mu_{b,1})'$ from the above multivariate distribution, if the generated value of $\mu_{a,1}$ or $\mu_{b,1}$ is less than or equal to 0, that draw is discarded, otherwise it is saved, this is in order to ensure that $\mu_{a,1} > 0$ and $\mu_{b,1} > 0$.

A.5 Drawing $\sigma_a^2, \sigma_b^2, \sigma_{ab}$ given $\mu_{0,a}, \mu_{1,a}, \mu_{0,b}, \mu_{1,b}, \tilde{S}_{a,T}, \tilde{S}_{b,T}, \tilde{S}_T, \tilde{V}_T$ and \tilde{y}_T

Conditional on the mean parameters, state variables and the data, by using the corresponding likelihood function, the conditional posterior distribution

$$p(\Sigma^{-1} | \tilde{S}_{a,T}, \tilde{S}_{b,T}, \tilde{S}_T, \tilde{V}_T, \mu, \tilde{y}_T),$$

takes the form

$$\Sigma^{-1} | \tilde{S}_{a,T}, \tilde{S}_{b,T}, \tilde{S}_T, \tilde{V}_T, \mu, \tilde{y}_T \sim W(\bar{S}^{-1}, \bar{v}), \quad (69)$$

where

$$\begin{aligned}\bar{v} &= T + v \\ \bar{S} &= \underline{S} + \sum_{t=1}^T (y_t - \bar{S}_t \mu) (y_t - \bar{S}_t \mu)',\end{aligned}$$

after Σ^{-1} is generated the elements of Σ are recovered.

References

- [1] Acemoglu D, Carvalho V M, Ozdaglar A, Tahbaz-Salehi A. 2012. The network origins of aggregate fluctuations. *Econometrica* 80:5, 1977-2016.
- [2] Anas J, Billio M, Ferrara L, Lo Duca M. 2007. Business Cycle Analysis with Multivariate Markov Switching Models. Working Papers, Department of Economics, University of Venice Ca' Foscari.
- [3] Artis M, Marcellino M, Proietti T. 2004. Dating Business Cycles: A Methodological Contribution with an Application to the Euro Area. *Oxford Bulletin of Economics and Statistics* 66:4, 537-565.
- [4] Bai J, Wang P. 2011. Conditional Markov chain and its application in economic time series analysis. *Journal of Applied Econometrics* 26:5, 715-734.
- [5] Bengoechea P, Camacho M, Perez-Quiros G. 2006. A useful tool for forecasting the Euro-area business cycle phases. *International Journal of Forecasting* 22:4, 735-749.
- [6] Boldin M D. 1996. A Check on the Robustness of Hamilton's Markov Switching Model Approach to the Economic Analysis of the Business Cycle. *Studies in Nonlinear Dynamics and Econometrics* 1:1, 35-46.
- [7] Cakmakli C, Paap R, Van Dijk D. 2011. Modeling and Estimation of Synchronization in Multistate Markov. Tinbergen Institute Discussion Papers 11-002/4.
- [8] Camacho M, Perez-Quiros G. 2006. A new framework to analyze business cycle synchronization. *Nonlinear Time Series Analysis of Business Cycles*. Elsevier's Contributions to Economic Analysis series. Chapter 5, 276, 133-149.
- [9] Camacho M, Perez-Quiros G, Saiz L. 2006. Are European business cycles close enough to be just one? *Journal of Economic Dynamics and Control* 30:9-10, 1687-1706.
- [10] Camacho M, Perez-Quiros G. 2007. Jump-and-rest effect of U.S. business cycles. *Studies in Nonlinear Dynamics and Econometrics* Vol. 11: No. 4, 3.
- [11] Carvalho V M. 2008. Aggregate Fluctuations and the Network Structure of Intersectoral Trade. Working Paper, CREI, 1977-2004.
- [12] Chauvet M, Senyuz Z. 2012. A Joint Dynamic Bi-Factor Model of the Yield Curve and the Economy as a Predictor of Business Cycles. Finance and Economics Discussion Series 32, Federal Reserve Board.
- [13] Crone T M, Matthews C. 2005. Consistent Economic Indexes for the 50 States. *Review of Economics and Statistics* 87:4, 593-603.

- [14] Dijkstra E W. 1959. A note on two problems in connexion with graphs. *Numerische Mathematik 1* 269–271.
- [15] Gabaix X. 2011. The Granular Origins of Aggregate Fluctuations. *Econometrica* 79, 733–772.
- [16] Goyal S. 2007. *Connections: An Introduction to the Economics of Networks*. Princeton University Press.
- [17] Guha D, Banerji A. 1998. Testing for cycles: A Markov switching approach. *Journal of Economic and Social Measurement* 25: 163-182.
- [18] Hamilton J D. 1989. A new approach to the economic analysis of nonstationary time series and the business cycle. *Econometrica* 57:2, 357-384.
- [19] Hamilton J D, Li G. 1996. Stock Market Volatility and the Business Cycle. *Journal of Applied Econometrics* 11:5, 573-593.
- [20] Hamilton J D. 1994. *Time Series Analysis*. Princeton, NJ: Princeton University Press.
- [21] Hamilton J D, Perez-Quiros G. 1996. What Do the Leading Indicators Lead? *Journal of Business* 69:1, 27–49.
- [22] Hamilton J D, Owyang M T. 2012. The Propagation of Regional Recessions. *Review of Economics and Statistics* 94:4, 935-947.
- [23] Harding D, Pagan A. 2006. Synchronization of cycles. *Journal of Econometrics* 132:1, 59-79.
- [24] Krolzing H. 1997. Markov-switching vector autorregresions. *Modelling, statistical inference and applications to business cycle analysis*. Lecture Notes in Economics and Mathematical Systems 454.
- [25] Kim C, Nelson C R, Startz R. 1998. Testing for Mean Reversion in Heteroskedastic Data Based on Gibbs-Sampling-Augmented Randomization. *Journal of Empirical Finance* 5:2, 131-154.
- [26] Kim C, Nelson C R. 1999. *State-Space Models with Regime Switching: Classical and Gibbs-Sampling Approaches with Applications*. MIT press.
- [27] Leiva-Leon D. 2014. Real vs. Nominal Cycles: A Multistate Markov-Switching Bi-Factor Approach. *Studies on Nonlinear Dynamics and Econometrics*. Forthcoming.
- [28] Owyang M, Piger J, Wall H. 2005. Business Cycle Phases in U.S. States. *Review of Economics and Statistics* 87:4, 604-616.

- [29] Pesaran M H, Timmermann A. 2009. Testing Dependence Among Serially Correlated Multicategory Variables. *Journal of the American Statistical Association* 104:485, 325-337.
- [30] Phillips K. 1991 . A two-country model of stochastic output with changes in regime. *Journal of International Economics* 31: 121-142.
- [31] Sims C A, Zha T. 2006. Were There Regime Switches in U.S. Monetary Policy? *American Economic Review* 96(1): 54-81.
- [32] Sims C A, Waggoner D F, Zha T. 2008. Methods for inference in large multiple-equation Markov-switching models. *Journal of Econometrics*. 146: 2, 255-274.
- [33] Smith P A and Summers P M. 2005. How well do Markov switching models describe actual business cycles? The case of synchronization. *Journal of Applied Econometrics* 20:2, 253-274.
- [34] Strogatz S H, Watts D J. 1998. Collective dynamics of 'small-world' networks, *Nature* 393:6684, 440-442.
- [35] Tim N H. 2002. *Applied Multivariate Analysis*. Springer texts in Statistics.
- [36] Xu K S, Klinger M, Hero III A O. 2012. A regularized graph layout framework for dynamic network visualization. *Data Mining and Knowledge Discovery* 27:1, 84-116.

Table 1: Parameter values for generating processes

Parameter	Value	Parameter	Value
$\mu_{a,0}^*$	-1	$\mu_{b,0}^*$	-2
$\mu_{a,1}^*$	2	$\mu_{b,1}^*$	4
$p_{a,11}^*$	0.9	$p_{b,11}^*$	0.9
$p_{a,00}^*$	0.8	$p_{b,00}^*$	0.8
p_{11}^*	0.9	$p_{V,11}^*$	0.9
p_{00}^*	0.8	$p_{V,00}^*$	0.8
σ_a^*	1	σ_b^*	1
$\sigma_{a,b}^*$	0.1		

Note: The table shows the parameter values used to generate the stochastic processes y_t in Equation (42) for the simulation study, in Section 2.2.

Table 2: Performance of parameters estimation

	$z = 1$	$z = 2$	$z = 3$	$z = 4$	$z = 5$	$z = f(V_t)$
$\mu_{a,0}^*$	-0.95143	-0.93985	-0.94558	-0.93750	-0.93166	-0.93896
$\mu_{a,1}^*$	1.91921	1.89427	1.90213	1.89147	1.88822	1.89089
$p_{a,11}^*$	0.89813	0.89689	0.89729	0.89606	0.89488	0.87803
$p_{a,00}^*$	0.79663	0.79508	0.79393	0.78997	0.78900	0.75626
$\mu_{b,0}^*$	-1.98915	-1.99861	-1.99591	-1.99903	-1.99503	-1.99729
$\mu_{b,1}^*$	3.98711	3.99662	3.99139	3.99859	3.99011	3.99148
$p_{b,11}^*$	0.89700	0.89576	0.89581	0.89341	0.89188	0.86977
$p_{b,00}^*$	0.79166	0.79155	0.79088	0.78574	0.78600	0.74422
p_{11}^*	0.89433	0.89241	0.89406	0.89026	0.88991	0.86936
p_{00}^*	0.78479	0.78295	0.78600	0.77786	0.78900	0.74178
$p_{V,11}^*$	—	—	—	—	—	0.89682
$p_{V,00}^*$	—	—	—	—	—	0.80971

Note: The entries in the table report the average of the estimated parameters values through the 1000 replications for different numbers of synchronization changes, z .

Table 3: Performance of regimes inference

	$z = 1$	$z = 2$	$z = 3$	$z = 4$	$z = 5$	$z = f(V_t)$
$QPS(S_{a,t})$	0.05118	0.06448	0.05571	0.06470	0.06023	0.06074
$QPS(S_{b,t})$	0.00749	0.00765	0.00763	0.00829	0.00805	0.00990
$QPS(V_t)$	0.06387	0.08554	0.09526	0.10988	0.11575	0.17769

Note: The entries in the table report the average of the Quadratic Probability Score associated to the state variables through the 1000 replications for different numbers of synchronization changes, z .

Table 4: Dynamic synchronization estimates between New York and Texas

	Mean	Std. Dev.	Median
$\mu_{ny,0}$	-0.12945	0.01856	-0.12895
$\mu_{ny,1}$	0.36121	0.01844	0.36079
σ_{ny}^2	0.02001	0.00153	0.01996
$p_{ny,11}$	0.98322	0.00744	0.98456
$p_{ny,00}$	0.93251	0.02667	0.93539
$\mu_{tx,0}$	-0.20619	0.02203	-0.20614
$\mu_{tx,1}$	0.56382	0.02258	0.56399
σ_{tx}^2	0.02605	0.00187	0.02593
$p_{tx,11}$	0.98503	0.00642	0.98598
$p_{tx,00}$	0.93265	0.02687	0.93487
$\sigma_{ny,tx}$	0.00819	0.00156	0.00820
p_{11}	0.98113	0.00775	0.98240
p_{00}	0.93069	0.02523	0.93472
$p_{V,11}$	0.96516	0.03974	0.97721
$p_{V,00}$	0.96206	0.02731	0.96879

Note: The selected example presents the case of two states with high and similar U.S. GDP share, New York with 7.68%, and Texas with 7.95%.

Table 5: Dynamic synchronization estimates between California and Vermont

	Mean	Std. Dev.	Median
$\mu_{ny,0}$	-0.05433	0.01651	-0.05441
$\mu_{ny,1}$	0.38183	0.01736	0.38236
σ_{ny}^2	0.02320	0.00180	0.02314
$p_{ny,11}$	0.97917	0.00855	0.98015
$p_{ny,00}$	0.94655	0.01969	0.94817
$\mu_{tx,0}$	-0.12031	0.02875	-0.11942
$\mu_{tx,1}$	0.44574	0.03106	0.44586
σ_{tx}^2	0.05672	0.00447	0.05647
$p_{tx,11}$	0.97762	0.00882	0.97884
$p_{tx,00}$	0.94139	0.02105	0.94373
$\sigma_{ny,tx}$	0.01574	0.00245	0.01561
p_{11}	0.97829	0.00895	0.97956
p_{00}	0.94627	0.02031	0.94897
$p_{V,11}$	0.97412	0.02714	0.98243
$p_{V,00}$	0.93864	0.03777	0.94518

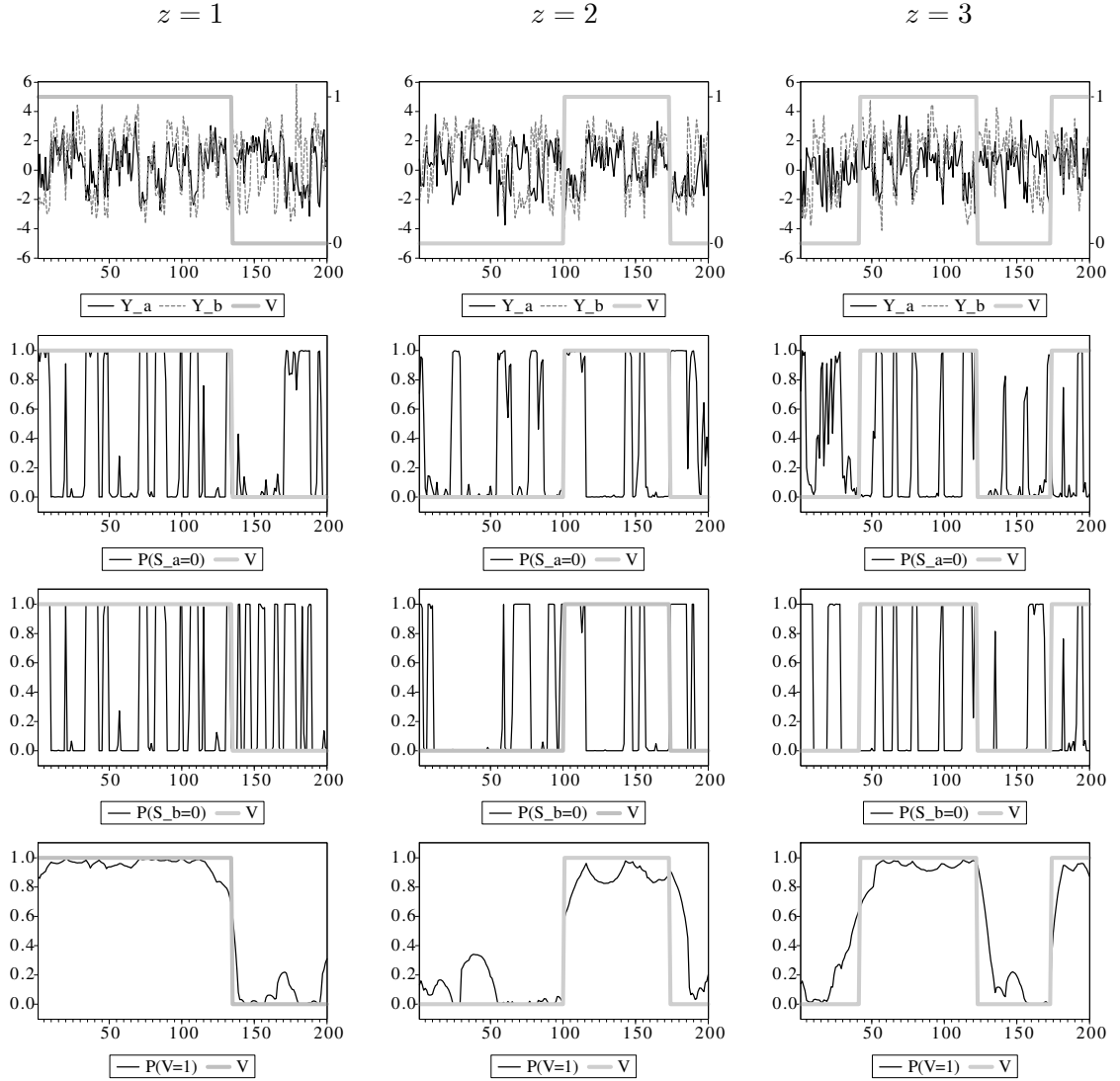
Note: The selected example presents the case of the states with the highest and the lowest U.S. GDP share, i.e. California with 13.34% and Vermont with 0.18%.

Table 6: Stationary synchronization between states and U.S.

State	Sync	State	Sync	State	Sync
Alabama	0.79	Maine	0.74	Ohio	0.84
Arizona	0.71	Maryland	0.52	Oklahoma	0.19
Arkansas	0.62	Massachusetts	0.56	Oregon	0.72
California	0.80	Michigan	0.85	Pennsylvania	0.79
Colorado	0.32	Minnesota	0.75	Rhode Island	0.65
Connecticut	0.79	Mississippi	0.75	S. Carolina	0.87
Delaware	0.77	Missouri	0.85	S. Dakota	0.54
Florida	0.70	Montana	0.34	Tennessee	0.84
Georgia	0.86	Nebraska	0.39	Texas	0.33
Idaho	0.57	Nevada	0.78	Utah	0.47
Illinois	0.75	N. Hampshire	0.44	Vermont	0.69
Indiana	0.83	New Jersey	0.77	Virginia	0.88
Iowa	0.59	New Mexico	0.49	Washington	0.69
Kansas	0.72	New York	0.72	Wisconsin	0.75
Kentucky	0.77	N. Carolina	0.91	W. Virginia	0.45
Louisiana	0.31	N. Dakota	0.24	Wyoming	0.25

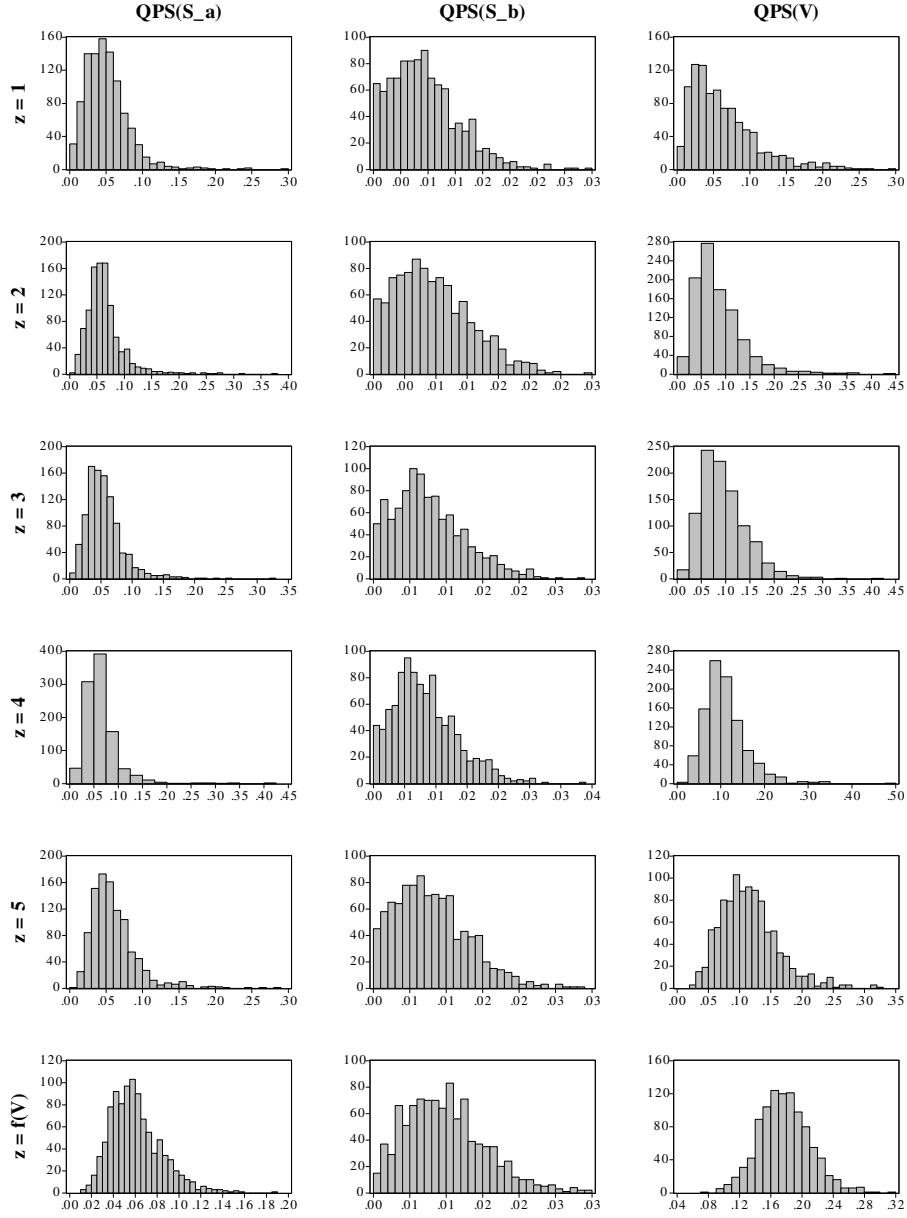
Note: The table reports the stationary synchronization for the period 1979:8 - 2013:3. Those estimates correspond to the ergodic probability that the phases of the state business cycles and U.S. business cycles are the same, i.e. $\Pr(V_t = 1)$. The index used to measure the national business cycle is the Chicago Fed National Activity Index (CFNAI).

Figure 1: Simulation of changes in synchronization of cycles



Note: The figure plots one simulations for the cases of 1, 2 and 3 changes in the synchronicity of cycles. For each case, the top panels plot the generated pair of time series along with the indicator variable of sync changes. The two middle panels plot the probabilities of low mean regime associated to each time series, along with the indicator variable as reference. The bottom panels plot the estimated dynamics of the indicator variable along with the real one.

Figure 2: Histograms of the performance of regimes inference

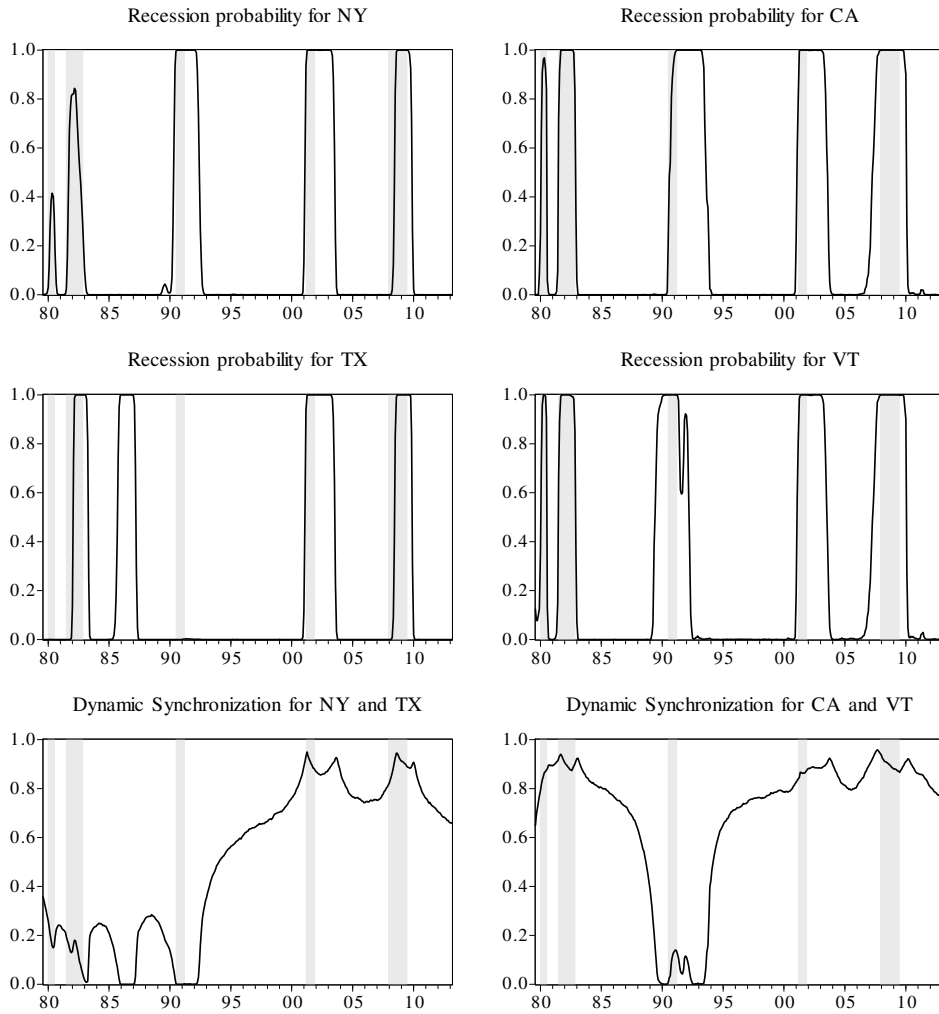


Note: The figure plots the histograms based on the 1000 replications of the Quadratic Probability Score associated to the state variables for different numbers of synchronization changes, z .

Figure 3: Dynamic synchronization between selected states

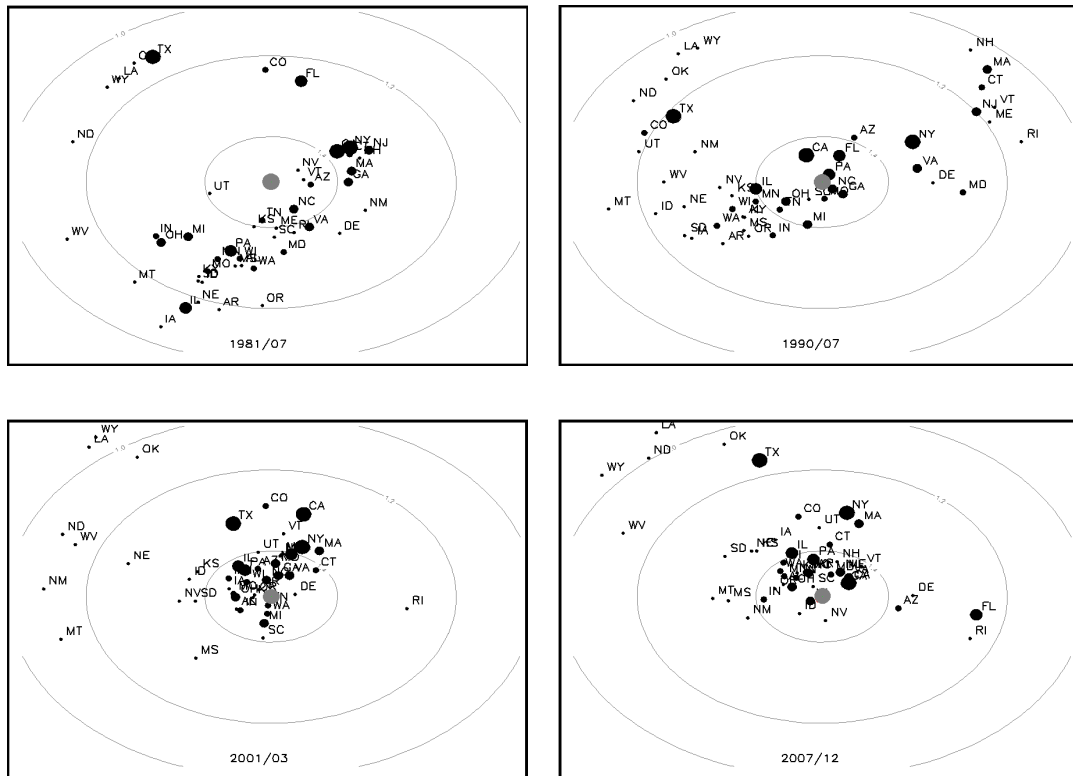
Chart A. New York and Texas

Chart B. California and Vermont



Note: The figure plots the output estimation for two selected pairwise models. Chart A plots the probability of recession for New York and Texas along with their dynamic synchronization. Chart B plots the probabilities of recession for California and Vermont along with their dynamic synchronization. Shaded areas correspond to NBER recessions.

Figure 4: U.S. states dynamic synchronization maps across recessions



Note: Each chart in the figure plots the dynamic multidimensional scaling map based on the sync distance of the U.S. states business cycle for different periods. The distances are normalized with respect to the U.S. national economic activity, the grey point in the center. The size of the points make reference to the GDP share of the corresponding state. If two states are placed in the same orbit, they are equally in sync with U.S. The full animated version of the synchronization mapping is available at: <https://sites.google.com/site/daniloleivaleon/media>

Figure 5: Grouping pattern based on business cycle phases

Chart A. U.S. states ergodic synchronization map

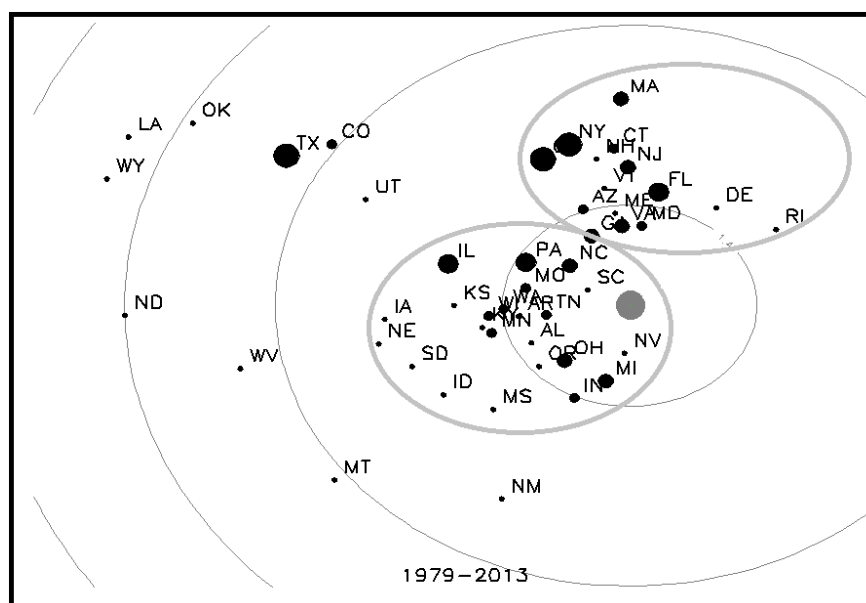


Chart B. Clustering patter obtained in Hamilton and Owyang (2012)



Note: Chart A plots the multidimensional scaling map based on the stationary sync distance of the U.S. States business cycle characteristics for the sample 1979:08- 2013:03. The distances are normalized with respect to the U.S. National Economic Activity, the grey point in the center. If two states are placed in the same orbit, they are equally in sync with U.S. The ovals just make reference to groups. The full animated version can be found at the author's web page. In Chart B, the shading for each state indicates the probability that such state belongs to any given cluster. Source: Hamilton and Owyang (2012)

Figure 6: Synchronization between states and U.S.

Chart A. Stationary synchronization

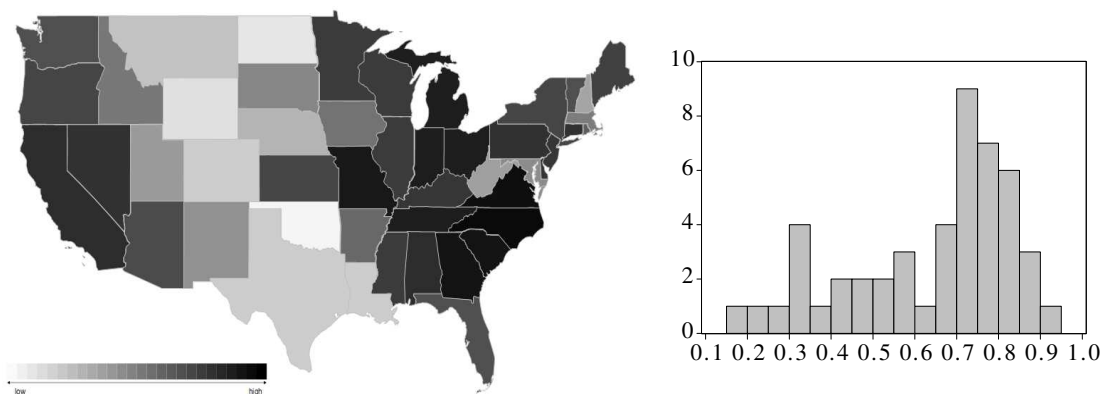
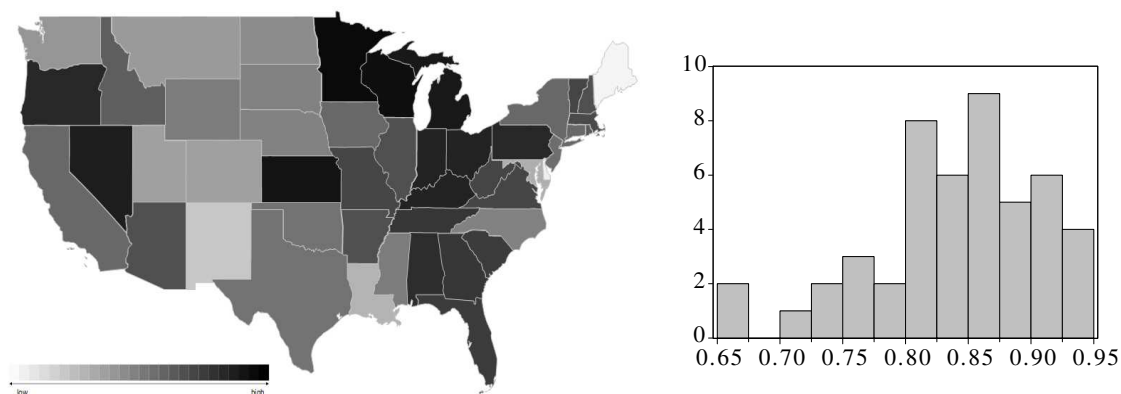
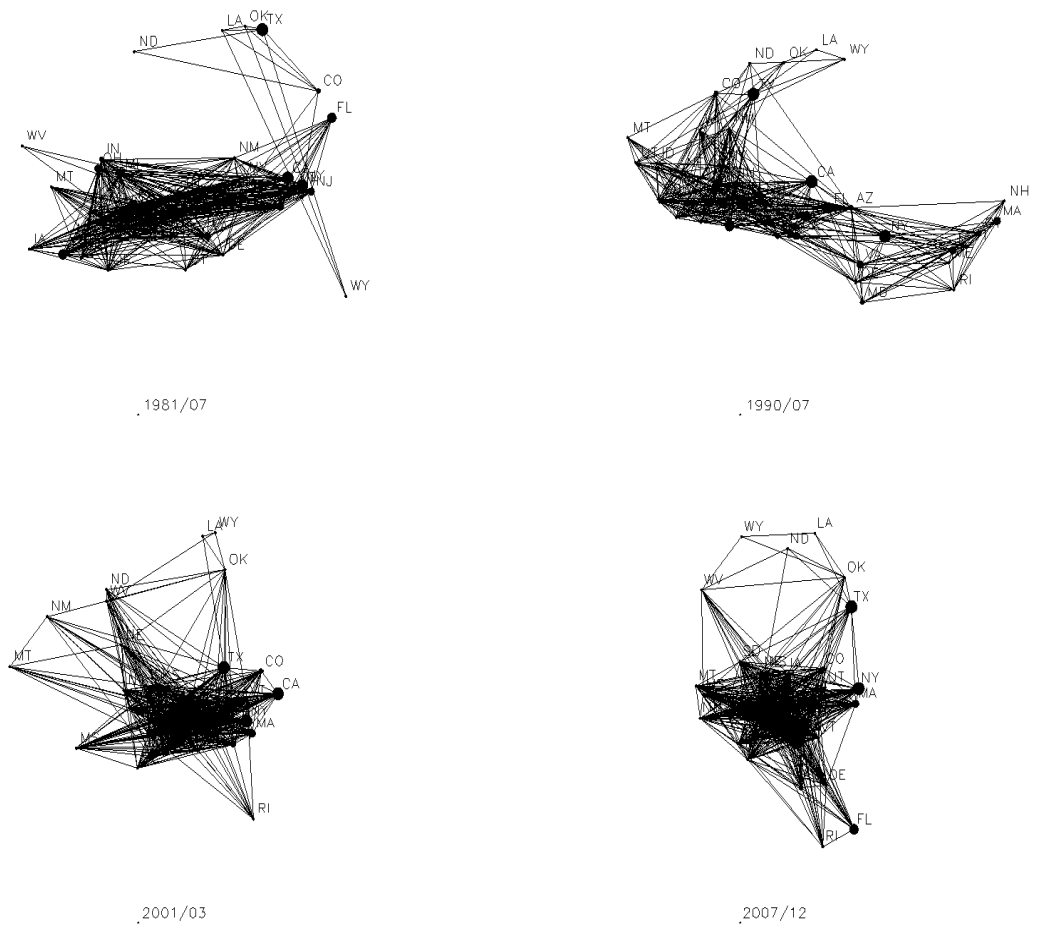


Chart B. Concordance based on Owyang et al. (2005)



Note: The Chart A of the figure plots a thematic map of the U.S. based on the stationary synchronization between each state and the national business cycle along with the histogram corresponding to data in Table 6, a darker state, presents a higher sync. The Chart B plots a thematic map of the U.S. by using the concordances obtained in Owyang et al. (2005) along with the corresponding histogram.

Figure 7: U.S. states synchronization network across recessions

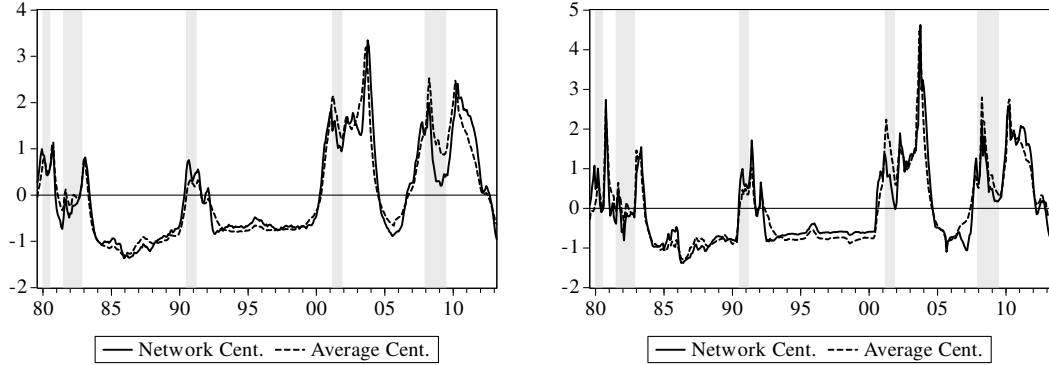


Note: The figure plots the interconnectedness in terms of synchronization between the business cycle phases of U.S. states. Each node represent a state and each line represents the link between two states, which take place only if $\Pr(Vt = 1) > 0.5$. The full animated version can be found at: <https://sites.google.com/site/danileivaleon/media>

Figure 8: Dynamic closeness centrality of U.S. synchronization network

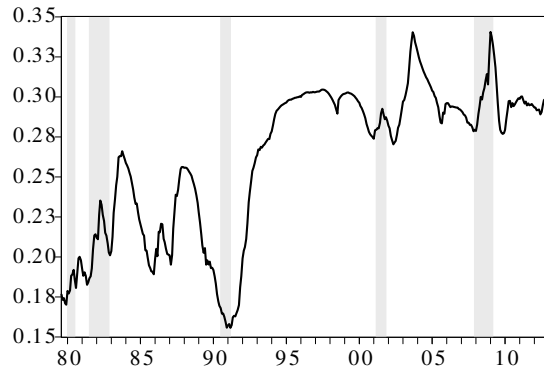
Chart A. Smoothed Prob.-based centrality

Chart B. Filtered Prob.-based centrality



Note: The Chart A of the figure plots the two measures of centrality of the Markov-switching synchronization network based on the smoothed probabilities, $\Pr(V_t = 1|\psi_T)$. The solid line plots the network closeness centrality defined in Equation (52) and the solid plots the average centrality as defined in Equation (53). The Chart B of the figure plot the same measures as in Chart A, but based on the filtered probabilities, $\Pr(V_t = 1|\psi_t)$. All the series in the figure are standardized to facilitate their comparison. Shaded bars refer to the NBER recessions.

Figure 9: Dynamic clustering coefficient of the U.S. synchronization network



Note: The figure plots the time-varying clustering coefficient of the Markov-Switching Synchronization Network for U.S. states. Shaded bars refer to the NBER recessions.